Pontifícia Universidade Católica
do Rio de Janeiro

**Luiz Umberto Rodrigues Sica**

# An experimental study of the validity of the von Mises yielding criterion for elasto-viscoplastic materials



**Tese de Doutorado**

Thesis presented to the Programa de Pós–graduação em Engenharia Mecânica of PUC-Rio in partial fulfillment of the requirements for the degree of Doutor em Engenharia Mecânica .

Advisor : Prof. Paulo Roberto de Souza Mendes
Co-advisor: Prof. Roney Leon Thompson

Rio de Janeiro
October 2017

Pontifícia Universidade Católica
do Rio de Janeiro

**Luiz Umberto Rodrigues Sica**

# An experimental study of the validity of the von Mises yielding criterion for elasto-viscoplastic materials

Thesis presented to the Programa de Pós–graduação em Engenharia Mecânica of PUC-Rio in partial fulfillment of the requirements for the degree of Doutor em Engenharia Mecânica . Approved by the undersigned Examination Committee.

**Prof. Paulo Roberto de Souza Mendes**
Advisor
Departamento de Engenharia Mecânica – PUC-Rio

**Prof. Roney Leon Thompson**
Co-advisor
Programa de Engenharia Mecânica - COPPE – UFRJ

**Prof. Márcio da Silveira Carvalho**
Departamento de Engenharia Mecânica – PUC-Rio

**Profa. Mônica Feijó Naccache**
Departamento de Engenharia Mecânica – PUC-Rio

**Prof. Edson José Soares**
Departamento de Engenharia Mecânica – UFES

**Prof. Fernando Alves Rochinha**
Programa de Engenharia Mecânica - COPPE – UFRJ

**Prof. Márcio da Silveira Carvalho**
Vice Dean of Graduate Studies
Centro Técnico Científico – PUC-Rio

Rio de Janeiro, October the 2nd, 2017

**Luiz Umberto Rodrigues Sica**

Luiz Umberto Rodrigues Sica graduated in Mechanical Engineering from Gama Filho University in 2010, with a full scholarship (Brazilian Ministry of Education). His final project won the Oscar Niemeyer Award for Scientific and Technological Works, CREA-RJ. Then, he started to work as a research engineer with computational modeling and numerical solution of partial differential equations, focused on thermo-hydro-mechanical-chemical processes in Geosystems, in the National Laboratory for Scientific Computing (LNCC), where he was already involved in research activities for 2 years and 5 months. After this period he had decided to start his master degree in computational modeling graduating as M.Sc. in Computational Modeling at the National Laboratory for Scientific Computing (LNCC) in February of 2014. In parallel in 2013, he had decided to change his research focus to rheological material characterization and continuum mechanics. Furthermore, he had stayed a year as a research fellow at Texas A&M University under professor Kumbakonam Rajagopal supervision.



Bibliographic data

Sica, Luiz Umberto Rodrigues

An experimental study of the validity of the von Mises yielding criterion for elasto-viscoplastic materials / Luiz Umberto Rodrigues Sica; advisor: Paulo Roberto de Souza Mendes; co-advisor: Roney Leon Thompson. – Rio de janeiro: PUC-Rio , Departamento de Engenharia Mecânica, 2017.

v., 91 f: il. color. ; 30 cm

Tese (doutorado) - Pontifícia Universidade Católica do Rio de Janeiro, Departamento de Engenharia Mecânica.

Inclui bibliografia

1. Engenharia Mecânica – Teses. 2. Critério de falha de von Mises;. 3. Materiais elasto-viscoplásticos;. 4. Tensões normais;. 5. Ensaio de compressão;. 6. Ensaio de tração;. I. de Souza Mendes, Paulo Roberto. II. Thompson, Roney Leon. III. Pontifícia Universidade Católica do Rio de Janeiro. Departamento de Engenharia Mecânica. IV. Título.

CDD: 621

## Acknowledgments

Initially, I would like to thank the architect of the universe for the grace of existing, and for the grit that was allowed to me. Only I know the suffering I have gone through and the countless sleepless nights working uninterruptedly. I would like to thank my family who has always been at my side, fighting side by side and going through many difficulties with me. Mrs. Diva Rodrigues Sica, my mother, I could not have wished for a more powerful guardian angel. Leonardo Rodrigues Sica, my brother, nor the title of doctor will make me as proud as the pride I have in being your brother. And for the patience, companionship, and affection of my love Tainá Ferreira de Lima.

I am very happy to say that during my Ph.D. studies, I did not have just co-workers but friends, and I will take it forever with me. I have so many names to thank regarding the students and staff of the Rheology Group of PUC-Rio, which I hereby record my thanks to everyone. To Bruno, my friend, for helping with the traction tests and has listened to me often when my work was not recognized and I had to deal with injustice. The patience of Alexandre, whom I often disturbed in order to machine the pieces of adaptation while I was developing countless other things in parallel. To Pedro and Elias, for have helped with the processing and plot the images. And to Roberta, for the patience and kindness in having taken up many experimental doubts at the beginning after my return from Texas, and teaching me how to operate the Haake rheometer on the first weeks after my return.

Lastly, I would like to thank CAPES, for the financial support which allowed this work to be done.

## Abstract

Sica, Luiz Umberto Rodrigues; de Souza Mendes, Paulo Roberto (Advisor); Thompson, Roney Leon (Co-Advisor). **An experimental study of the validity of the von Mises yielding criterion for elasto-viscoplastic materials**. Rio de Janeiro, 2017. 91p. Tese de doutorado – Departamento de Engenharia Mecânica, Pontifícia Universidade Católica do Rio de Janeiro.

It is usual practice in rheology to measure the yield stress in a simple shear flow. In these measurements, the yield stress is identified as the maximum value of the shear stress below which no irreversible flow occurs. Then, the thus determined yield stress is used in conjunction with the von Mises criterion in any complex flow. The latter compares it with the intensity of the deviatoric stress tensor. It happens that for simple shear flow the intensity of the deviatoric stress is composed of both the shear stress and the normal stress differences, but the contribution of the latter is never considered in the experimental determination of the yield stress. In view of assess the importance of the contribution of the normal stresses to the yield stress, a sequence o standard constant shear stress tests were performed for each material, estimating the critical stress which represents the mean value obtained between the stress values of the curves in which the material flows and does not flow with an accurate tolerance. After that, proposed tests were performed in order to obtain the values of $N_1 - N_2$ and solely $N_1$ at the critical stresses. Following the appropriate yield stress evaluation. It was observed that for some materials the normal stress contribution is much larger than the shear stress contribution. Furthermore, the validity of the von Mises yielding criterion for elasto-viscoplastic materials was evaluated. For this purpose, in order to generalize the study for different flow conditions, constant volume squeeze flow and traction tests were performed evaluating the corresponding yield stresses. As the most important conclusion, the von Mises yielding criterion was considered not to be accurate representing yielding for the elasto-viscoplastic materials analyzed.



## Keywords

von Mises yielding criterion; Elasto-viscoplastic materials; Normal stresses; Squeeze flow; Traction test;

## Resumo

Sica, Luiz Umberto Rodrigues; de Souza Mendes, Paulo Roberto; Thompson, Roney Leon. **Estudo experimental da validade do critério de falha de von Mises para materiais elasto-viscoplásticos**. Rio de Janeiro, 2017. 91p. Tese de Doutorado – Departamento de Engenharia Mecânica, Pontifícia Universidade Católica do Rio de Janeiro.

É uma prática usual em reologia medir o tensão limite de escoamento. Nessas medidas, a tensão limite de escoamento é definida como o máximo valor absoluto de tensão ao qual abaixo não ocorrem escoamentos irreversíveis. Sendo assim, tensão limite de escoamento aparente estimada é usada em conjunto com o critério de von Mises em qualquer escoamento complexo. Este critério compara esta medida a intensidade do segundo invariante do tensor deviatórico das tensões. Acontece que, para escoamento simples de cisalhamento, o mesmo é composto por tensões cisalhantes e diferenças de tensão normais, mas a contribuição do último nunca foi considerada na determinação experimental da tensão limite de escoamento. Em vista de avaliar a importância da contribuição das diferenças de tensões normais na tensão limite de escoamento aparente, foram realizadas uma sequência de testes de creep para cada material, estimando a tensão crítica que representa o valor médio obtido entre os valores das curvas de tensão nas quais o material escoa e não escoa com uma tolerância considerável. Depois disso, foram propostos testes para avaliar os valores de $N_1 - N_2$ e apenas $N_1$ no nível de tensão crítica. E em seguida avaliando-se adequadamente a tensão limite de escoamento. Observou-se que, para alguns materiais, a contribuição das diferenças de tensões normais é muito maior do que a contribuiçõ da tensão cisalhante. Por fim, a validade do critério de von Mises para materiais elasto-viscoplásticos foi avaliada. Para este fim, com o intuito de generalizar o estudo, ensaios de compressão a volume constante e de tração foram realizados avaliando-se as correspondentes tensões limites de escoamento. Como conclusão mais importante, o critério de von Mises não foi considerado adequado como critério de falha para os materiais elasto-viscoplásticos analisados.

## Palavras-chave

Critério de falha de von Mises; Materiais elasto-viscoplásticos; Tensões normais; Ensaio de compressão; Ensaio de tração;

# Table of contents

# List of figures

# List of tables

*"The mediocre teacher tells. The good teacher explains. The superior teacher demonstrates. The great teacher inspires."*

**William Arthur Ward**

# 1
# Motivation

In nature and in several industrial applications there is a huge variety of materials with elasto-viscoplastic characteristics, in which the time dependent behaviour could be observed. In the follow paragraphs we will cite some examples to emphasize the importance of developing models for those materials.

The discs of the human spine show this kind of behaviour. Under the action of body weight, the discs slip on each other, ie they become shorter over time. At bedtime allow the recovery of the spinal discs and this means that most people are higher in the morning than during the night.

The skin tissue is another example. This can be seen by pressing and pulling the skin; It takes a while to recover and return to its flat original position. The skin is pulled over, more recovery time is needed. The faster pull, less time is required for recovery (It behaves "more elastic"). The skin is a material that ages, i.e., its physical properties change over time. Younger skin recovers more quickly than older skin.

Wooden beams of old houses, as observed, show distortions, however, this slip due to the weight of the structure and gravity can take several decades or even centuries to be noticed. Concrete and soils are other materials that tend to suffer landslides, as well as ice, and this with direct consequences in glacial movements.

Materials that behave elastically at room temperature will often reach significant viscoelastic properties when heated. For example, the metal turbine blades in jet engines, which reach very high temperatures and have to withstand very high stresses. Normally metals can suffer landslides at high temperatures and this led to the development of different materials. Currently, turbine blades are manufactured as superalloys containing any or total nickel, cobalt, chromium, aluminum, titanium, tungsten and molybdenum.

In the petroleum industry, the processes such as drilling and completion of wells involve the disposal, replacement and the displacement of non-Newtonian fluids. Very often the fluids involved have viscoplastic mechanical behavior as suspensions and emulsions. During these processes occur several phenomena (thixotropic, for example) that need to be clarified and that are often crucial to the success of the operation.

There are several foods in the food industry with viscoelastic properties. For example, the bread dough is a viscoelastic food. The wheat's ability to produce a viscoelastic mass can be explained by the behavior of amorphous gluten proteins.

There are several examples of materials which shows a time dependent behaviour include emulsions, paints, nanocomposites, gels, drilling fluids, food products ans mineral slurries. These materials in generally consist of dispersions whose microscopic characteristics generate a microstructure that governs their macroscopic behaviour in response to an applied stress. In the first time you faced this modeling problem, if you look in a quantitative perspective seems like the variety of intrisic charactheristics and a possible complex combination of components in a material would lead to an unmeasurable number of rheological behaviour types. But, according to (25), in a qualitative point of view, these materials show a limited and finite number of rheological behaviour types, the reason for it is that the interactions among the local elements of the material are similiar for different kinds of materials.



## 1.1 Research objective and thesis overview

A standard definition of a yield stress material is a material which behaves in a rigid body motion unless the deviatoric stress tensor satisfies a yield criterion (34). When the critical stress determined by the yield criterion is surpassed, the sample exhibit plastic effects (25). It is common for Non-Newtonian models to implicitly incorporate an isotropic yield criterion (see for example (95)), specifically the von Mises criterion (work published in (87), see also (48)), which is widely accepted as appropriate for material characterization in rheology. It is usual practice in rheology to measure the yield stress in a simple shear flow. In these measurements, the yield stress is identified as the maximum value of the shear stress below which no irreversible flow occurs. Then, the thus determined yield stress is used in conjunction with the von Mises criterion in any complex flow. The von Mises criterion compares it with the intensity of the deviatoric stress tensor, i.e. the square root of the absolute value of the deviatoric stress tensor second invariant. It happens that for simple shear flow the intensity of the deviatoric stress is composed of both the shear stress and the normal stress differences, but the contribution of the latter is never considered in the experimental determination of the yield stress. In view of assessing the importance of the contribution of the normal stresses to the yield stress, in the first part of the present research at chapter 3, a sequence o standard creep tests were performed for each material, estimating the critical

stress ($\sigma_{21,y}$) which represents the mean value obtained between the stress values of the curves in which the material flows[1] and does not flow with an accurate tolerance[2]. After that, shear stress ramps were performed using two different geometries (cone-plate and parallel plates). The sandblasted cone and plate geometry was employed to evaluate $N_1$ behavior as a function of applied stress, and consequently, the threshold value $N_{1,y}$ which corresponds to the critical stress $\sigma_{21,y}$. Additionally, the same procedure was adopted with a parallel cross-hatched plates which have given the behavior of $N_1 - N_2$ as a function of the applied stress, and the threshold value $N_{1,y} - N_{2,y}$, what enabled us to estimate $N_{2,y}$.

Furthermore, in the last part of the present work at Chapter 4, the validity of the von Mises yielding criterion for the materials under study was analyzed. For this purpose, traction and constant volume squeeze flow measurements were performed evaluating their corresponding yield stresses. Discrepancies were encountered for the estimated yield stresses for simple shear, traction, and squeeze flow, due to the fact that all results should be the same regardless the type of flow.

Summarizing, this thesis is organized into six chapters. As previously established, chapter 1 has presented the motivation of this research, with several examples of materials with time-dependent behavior emphasizing the importance of modeling them, and the objectives of this work. In chapter 2, the literature review has received a special attention, non-Newtonian behavior aspects and a brief introduction to yielding criteria were presented with a special emphasis on normal stresses. The first part of the present research was described in Chapter 3 in which the importance of the contribution on the normal stresses on the determination of the yield stress in a simple shear flow was studied. In Chapter 4, the study was extended for traction and compression flow conditions in which the validity of the von Mises yield criterion for the elasto-viscoplastic materials analyzed was evaluated. Lastly, chapter 5 and 6 were dedicated to the final remarks and bibliography.



[1]By the time the strain rate starts to increase it indicates that the material is starting to deform.

[2]Related to the small difference in Pa of the considered stresses.

# 2
# A brief review on Rheology and an introduction to yield criteria

The divergence of opinions about the existence of yield stress, time dependence behavior, confusion between thixotropic and shear thinning phenomena description, normal stresses in shear, the vast amount of models available in the literature and the several different ways to approach modeling the Non-Newtonian behavior are the main reasons that we have considered important the following brief review.

## 2.1
## Thixotropy, shear thinning and viscoelasticity



We must act carefully when describing the differences between thixotropy and shear thinning since in the literature a lot of scientists have confused these physical phenomena (see examples in (10)). This chapter will be dedicated for a brief review about “what we understand as thixotropy" based in (10, 85, 28) and by the end of this section point out the differences between the recent definition of thixotropy, shear thinning and viscoelasticity.

Everything has started with the discovery that gels had the property to become liquid-like by “shaking" such physical behavior was known for temperature changes. Specifically, according to (10), Schalek and Szegvari were the scientists (working in H. Freundlich’s laboratory) who found out, when they were studying aqueous iron oxide, that these sols were liquified by shaking and solidified again after a period of time (see (112)). With these results, they showed that sol-gel transitions could not only be induced by changes in temperature but also by means of an isothermal mechanical agitation (85). The group of researchers at H. Freundlich at the Kaiser Wilhelm made very important contributions in the study of this phenomenon (38). I little later, during the 30s and 40s countless different materials were discovery to display similar behavior (see for example (38, 44, 45, 78)).

According to (85) the term “thixotropy" (combination of the words thixis: shaking and trepo: changing, see (118)) was introduced by (37), based on a suggestion of (121). One explanation of thixotropy was proposed by (104) “an increase of viscosity in a state of rest and a decrease of viscosity when submitted

to a constant shearing stress [*sic*]" but this definition did not mention the time-dependent behavior of the material. An example of confusion between the time-dependence and shear rate dependence (see (85)) is the definition provided by (42) "an isothermal reversible decrease of viscosity with an increase of shear rate [*sic*]" by definition, this is not correct because this sentence described what we consider as shear thinning.

Good definitions for thixotropy and shear thinning were provided by (53): "If the viscosity is an unvalued function of the rate of shear, a decrease of the viscosity with increasing rate of shear is called shear thinning, and an increase of the viscosity shear thickening. (...) The application of a finite shear to a system after a long rest may result in a decrease of the viscosity or the consistency. If the decrease persists when the shear is discontinued, this behavior is called work softening (or shear breakdown), whereas if the original viscosity or consistency is recovered this behavior is called thixotropy." This definition is directly related with reversible (except for work softening phenomena, (53, 86)), time-dependent, and flow-induced change in viscosity (86), It is worth noting the important effect of recovery of viscosity when the flow is discontinued.

In general, a simple way to describe those definitions is given a sample and specific flow conditions some material response behaviors can be observed as the shear rate increases: (i) a decrease in viscosity (shear thinning) or (ii) an increase in viscosity (shear thickening); a time-dependency, (iii) the viscosity decreases over time (thixotropy) or (iv) increase (rheopexy). It is worth noting that these ideal material behaviors in reality do not exist isolated, but they help to simplify the phenomena in order to develop an approximate model.

As pointed out by (97), in respect to polymers viscoelasticity, depending on the timescale (or speed) of the deformation that the molecules undergo, at any temperature, it cannot be considered liquid either solid, but viscoelastic. A dimensionless number, called *Deborah number*[1] (107) and the deformation can be used to help us giving an insight about in which microstructural situation the material is passing through. In the polymer case, at small Deborah numbers it can be modeled as a Newtonian fluid and at high Deborah numbers as a Hookean solid, in between, we have the "viscoelastic region" that could be divided in two parts related to the applied deformation: small deformations (linear viscoelastic region) and large deformations (nonlinear viscoelastic region) (see chapter 5, (97)). The rise of nonlinearities is related to the fact that with large enough deformations polymers chain microstructure

[1]It is defined as the ratio between the relaxation and experimental observation times. This name was chosen by Marcus Reiner (see (107)) because of the Bible passage often called "Song of Deborah" (Judges 5:5), which states "The mountains flowed before the lord".

can be altered. As thixotropic systems, linear viscoelastic systems show time-dependent behavior in the sense that the microstructure takes time to respond to the applied stress, in other words, at shortimes[2] we see an elastic response. As reported by (10) both linear viscoelastic and thixotropic system have time effects, the first one is in the linear region, where the microstructure responds but remains unchanged[3] and the latter is in the non-linear region, when the microstructure is broken down by deformation as well responding to it.

Materials in which not only does the microstructure take time to respond to the flow, but it also changed by the flow and this change will itself take time are called nonlinear viscoelastic materials (10). (86) commented that "It has been argued in the literature that thixotropy is simple a type of nonlinear viscoelasticity and does not require separate treatment [*sic*]". Both nonlinear viscoelastic and thixotropic materials show time-dependent behavior, as for example overshoot stress in start-up flows, but as reported (86) some specific features of each phenomenon are neglected in models available in a literature, specifically, normal stress differences and stress relaxation in thixotropic models; and for polymers the gradual growth in stress after a drop in shear rate in nonlinear viscoelastic models. In reality, we do not have a "pure" material behavior, a majority of thixotropic materials show some degree of viscoelasticity and the definition of thixotropy does not exclude viscoelasticity. Actually, we have a general response[4] including a sudden drop and gradual stress relaxation, followed by a thixotropic recovery (see figure 7.1 at chapter 7 of (86)).



## 2.2 Yield stress

A good way to start this topic is defining microstructure. In general, the term microstructure is associated with the way in which particles are associated with each other in a material, but as reported by (10) It can also mean fibers' alignment, favorable spatial distribution of particles, drops or molecular associations in polymer solutions. The relation between thixotropy and the microstructure was well described by (10) in the following statement "(...) all liquids with microstructure can show thixotropy, because thixotropy only reflects the finite time taken to move from any one state of the microstructure to another and back again, whether from different states of flow or to or from

[2]high frequencies, see (10).

[3]It is not correct to apply the word unchanged, in fact, because of the small deformation applied, in a sliding plate rheometry for example, the microstructure remains almost unaffected in each cycle during the experiment (97).

[4]Considering an experiment with a drop in shear rate.

rest. The driving force for microstructural change in flow is the result of the competition between break-down due to flow stresses, build-up due to in-flow collisions and Brownian motion [*sic*]."

An important point with respect to model thixotropy is the concept of yield stress, defined by (128) as the stress, on a stress-strain curve, at the yield point in which above the deformation is not completely recoverable. Polymer compounds may recover their original dimensions completely as long as they are not stretched beyond the yield point. We can find in a literature a vast divergence of opinions about it. In the following paragraphs, we will summarize the main arguments in favor and against the yield stress concept, based on a reach discussion provided by (29).

It can be considered the article entitled "The yield stress myth" (12) the trigger of the opinion controversy. In this work, the authors defended that the yield stress does not exist as we can see in this quote "if the material flows at high stresses, it will also flow, however slowly, at low stresses [*sic*]". Later, supporting this idea plenteous arguments were provided by (11) in his review. Based on experimental results using the new generation of rheometers, he proves the inexistence of yield stress in various materials which were supposed to possess it, but in fact, those results were not a universal disproof of the existence of yield stress.

At this point, it is worth to define an expression well known from experimentalists, the "apparent yield stress". According to (29), it is define as, in a steady state, "a value in which below the materials flows like a Newtonian fluid with a very high (but finite) viscosity, in other words, in the range of small shear rates (and below the apparent yield stress), a high-viscosity Newtonian plateau appears in the flow curve". However, It is worth noting that the measure of the apparent yield stress must be done carefully because the value obtained depends on the analytical technique used.

Returning to the topic of discussion, some scientists have argued against (11) based on experimental results. Immersing a nylon sphere in a Carbopol® aqueous solution, the density of the sphere was slightly higher, (49) have concluded that the yield stress is an "engineering reality" based in the fact that after four months the sphere "did not move" (within 1 mm accuracy), similar experiments and conclusion can be found in (113). It is worth noting that in the same way that the experimental results provided by (11) were not a universal disproof of the existence of yield stress, the experimental results provided by (49, 113) were not either a universal proof because theoretically we would need a experiment with infinity observation time to prove it, even with better accuracy it would be an evidence and not a universal proof.

The divergence of opinions about yield stress still stands, since it is possible to find in a recent literature, papers defending the existence of yield stress. It is worth mentioning, after this brief review, the point of view provided by (6). In this work, he defended the idea that yield stress should be seen as an assumption that could be useful for some problems, as incompressibility for fluids. Lastly, complementing this point of view, there is an interesting comment provided by (29) "If the necessary precautions are taken, the yield-stress assumption can be used to model real fluids, and it is known to provide a realistic description for a wide variety of engineering applications (...)".

## 2.3 Normal stresses

A non-limited form to introduce this topic, commonly adopted in the literature is describing the well known rod-climbing phenomenon also known as Weissenberg effect, which is another Non-Newtonian behavior evidence[5]. If we prepare an experimental apparatus in which a rod rotates steadily in a container, the sample could display two qualitative behaviors: (i) for a Newtonian sample, the material is pushed outwards by centrifugal forces[6] (14) causing a depressed free surface near to the rotational rod; (ii) for a Non-Newtonian liquid with measurable normal stresses (33), the sample moves in the opposite direction toward de the rod and climbs it up, it is worth mentioned that the free surface can rise amazingly. This phenomenon was first described by (110) and (39), but according to (14), it is been known previously[7] in the paint industry. For further details, see the book (33) which in its section 2.2 presents a set of Weissenberg effect photographs for different Non-Newtonian fluids[8]. It is important to emphasize that the Weissenberg effect is an unstable phenomenon with random changes in the free surface profile, varying from stable and modest forms for elastic liquids to extremely unstable and random for highly elastic and shear thinning polymer solutions.

The first detailed scientific study on this phenomenon was carried out by Dr. K. Weissenberg (127) who performed experiments with several Non-Newtonian fluids in his pioneer analysis, under Dr. C. H. Lander from de Institute of Fuel supervision. Furthermore, in his work, he proposed his well-known hypothesis in which the second normal stress difference should be considered precisely zero, even known that the scientific community has shown

[5]However, as will be commented later some Newtonian fluids can display such behavior.

[6]It is worth to note that centrifugal forces are not forces by definition, just observed in a non-inertial rotating frames with respect to an inertial frame can perceive it (52).

[7]Related to its description in the scientific literature.

[8]Fiber suspensions, highly elastic and shear thinning polymer solution and weak elastic liquids.

that it is not correct still a good first approximation for some problems (14). It is enriching to cite the physical description given to this phenomenon by Dr. K. Weissenberg, "(...) If, as in our experiments, the lines of flow are closed circles, the pull along these lines strangulates the liquid and forces it inwards against the centrifugal forces and upwards against the forces of gravity. (...)".

A great effort has been done by the scientific community on normal stresses measurements and modeling since the pioneering work of Dr. K. Weissenberg. A brilliant and inspiring work was published by (2), in which the researchers have developed a cone-and-plate and parallel-plate rheometer-like machine in order to measure the normal stress differences in steady shear flow. (129) verified that the Weissenberg hypothesis was not correct, besides it was shown that at low shear rates $N_1$ and $N_2$ have the same sign. Some theoretical models available in the literature (83, 81, 89, 8) have proposed relationships between the first normal stress difference and shear stress, based on experimental data for polymer extrudate swell experiments which consist in a polymer extrudate through a metal conduit with constant cross section[9]. It is important to mention that a rigorous validation comparing the theoretical prediction and experimental data was performed by (89) and (8), strictly to low shear stresses. (18) has suggested a rheooptical method using a slit of rectangular cross-section to calculate the first normal stress differences of polymers at high shear stresses, the predictions have agreed satisfactorily with previous commented theoretical models predictions based on swelling ratios. The temperature influence on normal stresses measurements was analyzed by (114), using an interference method (proposed by (58)) which consists of a torsion flow contactless method of investigation that uses the epoxy resin intrinsic property of changing the refraction index when is undergoing a change in load and the interference of a large path difference. He has concluded that the normal stresses measured with this method are highly sensitive to a temperature gradient, and this method is applicable just with a sufficiently short time when the temperature gradient is negligible.

Even known that the scope of the present work is related to elasto-viscoplastic materials it is worth mentioning that the Weissenberg effect has been previously reported happening on dilute and semi-dilute fiber suspension in Newtonian fluids (92, 84, 109, 47). Although the constitutive theories for those fluids can predict steady shear and extensional viscosity, according to (133) they do not predict $N_1$. For further information, a detailed study on fiber suspension in Newtonian fluids can be found in (133), in which N1 was

[9]When a highly-elastic polymers exit the narrow conduit they show a behavior called die swell in which the fluid diameter becomes larger the conduit diameter itself.

measured for rigid glass fibers samples with different aspect ratios, to be sure the wall effect has not affected the data they have varied the gap using parallel plate geometry. Several constitutive theories were tested and just the equation derived by (21) showed adequate predictions for $N_1$ in a steady state shear flow. Lastly, a physical explanation of the Weissenberg effect for fiber suspension was given by (23) he said that "It might be that the shear flow between the glass fibers induces tensile stresses. The fiber tensile stresses acting along closed streamlines act as a normal stress in the fluid and induce the Weissenberg effect. (...)".

Several experimental studies were performed during the 60's and 70's, analyzing mainly polymers using Weissenberg rheogoniometer or equivalent experimental equipment collecting valuable data, as an example, we could cite the works (60, 43, 103, 35, 98, 63, 94), it is worth to mention the several contributions made by Dr. Alexander Malkin from the Institute of Petrochemical Synthesis at Moscow and co-workers (67, 126, 73, 125, 75, 124, 74). A normal stress correlation with a very good agreement for polyisobutylene fluids based on data available in the literature was proposed by (122). Although, as pointed out by him, the accuracy of the available data was not high, the author proposed an empirical correlation involving $N_1$ as a very weak function of the concentration (c), molecular weight (M) and shear stress, represented by $\frac{N_1 c^2}{|\sigma_{21}|^2} = 1.2 \times 10^{-5}(cM/10^6)^{0.13}|\sigma_{21}|^{-0.1}$. It is impressive the accuracy for polymers and the wide range of: (i) concentration ($1\% < c < 100\%$), (ii) molecular weight ($9 \times 10^4 <$M$< 15 \times 10^6$) and shear stress ($2$ Pa $< \sigma_{21} < 3.1 \times 10^4$ Pa). But it is important to mention the limitations founded, it fails for very small stresses and inaccurate results were obtained for very low molecular weights. Furthermore, analyzing the available $N_2$ data that was fragmented compared to $N_1$ data, according to the author, he came up with the following empirical correlation between $N_1$ and $N_2$, $N_2 \sim -0.15N_1$. (1) have proposed a relation based on Goddard-Miller rheological equation (41) to estimate $N_1$ from viscosity data, including at low shear rates, in which in order to obtain numerical results had introduced dimensionless quantities, the Carreu viscosity equation (20) was assumed to hold, and the subroutine ROMBRG[10] was applied to solve numerically the relation's improper integral. The equation was validated with ten materials[11] and, as the main purpose of their work, they had produced reasonable estimates[12] that intended to help design engineers who had just

[10]It is available on file at the Engineering Computing Laboratory of the University of Wisconsin.

[11]Six polymer melts, three polymer solutions, and an aluminum soap solution.

[12]It will comment later in this section based on the work (3) which had analyzed this method and others that it fails and produce inaccurate estimates of $N_1$.

viscosity data in hands. (75) considering viscoelastic polymers have studied the relaxation of $N_1$ after the cessation of steady shear flow, they proposed a method and validated it with experimental data, but it is important to mention that this method cannot reliably determine the first normal stress difference data for low time values.

Several theoretical normal stresses relationships for die swell available in the literature were analyzed by (124). They have concluded that the models with a better agreement with experimental data were the ones in which the dependence of the effective viscosity and viscoelastic deformations on the rate of deformation were neglected. (24) published a detailed theoretical work for several types of nonsteady shearing motions, it was shown that there are simple universal asymptotic relations between the shear stress and the first normal stress difference considering the general theory of incompressible simple fluids with fading memory. The co-rotational model of Le Roy-Pierrard, which is based in the Boltzmann's principle, was experimentally verified by (7) that have used an NBS polystyrene sample and a 50% by weight solution of polyisobutylene in mineral oil in a modified Weissenberg rheogoniometer. They could observe that two samples data had satisfied Yamamoto's equation. Furthermore, the NBS sample (with narrow distribution in molecular weight) displayed a simplified behaviour in which $N_1$ and $N_2$ decay at the same relative rate, that causes a situation in which the two memory functions of the model are not independent, and in this case the first memory function can be approximated by a single exponential.

A famous modified version of FENE model (120, 54) for dilute polymers was proposed by (15), known as FENE-P model in which the molecules were modeled as bead-spring chains considering the springs finite extensible, Oseen tensor (31) was used as in Zimm theory (132) to account the hydrodynamic interaction among the beads. This model was validated with the data available in the scientific literature. However, it is important to emphasize that comparing the values of $N_1$ estimated by FENE-P with the available data showed that the results were completely off and the authors commented that they were unable to explain the reason for it. (96) validates with experimental data the Doi-Edwards theory which consists of the *de Gennes*' tube model of entangled polymer chains. After has factored the total stress as $\boldsymbol{\sigma} = \boldsymbol{\gamma} h(\gamma) G(t)$, he has observed that the $h(\boldsymbol{\gamma})$ component agreed with this theory over a certain range of a long time, a limiting factor of this theory is that it is not applicable over a short time range which restricts the normal stresses predict capability. (5) used samples[13] of cis-l,4-Polybutadiene under small amplitude oscillatory

[13]They have not specified how many samples were used.

shear flow to validate Rouse molecular theory. But as they pointed out the measurements of the first normal stress differences were not accurate, besides thermal instabilities, due to the room, had affected the data meanly the normal forces measurements.

An interesting study was performed by (9), in which the reasonability of the choice of hole or exit pressure to measure $N_1$ in a slit-die apparatus was analyzed. Three polymer melts were tested in the later apparatus, comparing the results with the Higashitani-Pritchard (H-P) theory and results obtained using a cone-and-plate device. A good agreement among them could be obtained when the variable of choice was the hole pressure, but discrepant results appeared when the analysis was made with the exit pressure, estimating $N_1$ two to five times higher than the cone-and-plate estimate. Although the authors have made comments about the necessity of an improved pressure measurement technique, they had concluded that seemed reasonable to use the hole pressure and H-P theory to obtain $N_1$ values and the choice of the exit pressure was questionable.

Analysis on correlations between $N_1$ and shear stresses available in the literature, previously commented, were made by (3) using $N_1$ data from 32 different polymers solutions[14]. According to the authors, an excellent agreement was obtained by the relation proposed by (122), over the entire range of shear stresses adopted. In another hand, the relation proposed by (1) did not produce accurate predictions of $N_1$ from viscosity data, they had related this fact to the necessity of numerical integration with an extrapolation of the viscosity to infinitely high shear rate. The last analysis was made over FENE-P theory (15), it was very restrictive and did not follow the polymer solvent behavior. Besides, the model overestimates the data in the entire range of shear rate considered, showing serious drawbacks of this model. Lastly, the authors have proposed an empirical relation which has fitted satisfactorily the data, it was based on a dimensionless representation that FENE-P model suggested.

An extremely important discovery has been reported in the literature, it was found negatives values of $N_1$ for several materials and a similar qualitative behavior could be observed (56, 57, 91, 88, 76, 62). Traditionally, it was assumed for the entire range of shear rates that $N_1$ is null or positive. However, positive values of $N_1$ were found at low and high shear rates, with negative values occurring at intermediate shear rates. The first experimental report of this phenomena was published by (56), analyzing concentrated solutions

[14]It is important to mention that the $N_1$ data has been correlated to the shear stress by a simple Power-law model.

of Poly($\gamma$-Benzyl-Glutamate), they have observed negative values of $N_1$ in the intermediate shear rate values of the considered range. In order to be certain about the negative data obtained, they had applied the correction related to inertial forces which are known for producing spurious negative sign reversal (61). The values of the correction were much smaller than the measured values of $N_1$. The latter study was extended in (57), in which several concentrations of poly-$\gamma$-benzyl-L-glutamate and poly-$\epsilon$-carbo-benzyloxy-L-lysine were considered. The same trends[15] could be observed and an analysis of the influence of the concentration of the solutions on $N_1$ measurements was made. They had observed that the mechanisms responsible for both the first positive and the first negative regions of $N_1$ decrease in effect as the concentration is reduced.

The first theoretical work in which an intuitive and detailed discussion on the sign variation on $N_1$ was provided by (76), they had connected this variation with the direction of average molecular orientation tumbling[16] tendency under shear flow. Besides, a model that accounts this phenomenon was proposed. Their rich two-dimensional analysis can predict the sign variation of $N_1$. Although an accurate agreement was not possible comparing the theoretical predictions to the experimental data, the model was capable of predicting qualitatively the range in which $N_1$ is negative, the dependence on the polymer concentration and asymptotic plateaus. This work was generalized by (62), he had considered the problem in three dimensions[17], removed the previously used approximations and examined in more detail the process in which tumbling is arrested. He could observe the main conclusion of the previous work that shearing at a high enough rate can significantly distort the orientation-distribution function, making it less anisotropic. The $N_1$ sign behavior observed by his model were in qualitative agreement with the experimental data previous commented. Furthermore, he could also predict $N_2$ that was much smaller in magnitude than $N_1$ and in opposite sign, except in a specific small region in which the steady-state values of $N_1$ and $N_2$ were both negative. (4) had investigated $N_1$ and crystallization in a dense granular fluid. Although no experiments either comparisons with the available data were done, they had analyzed the validity of the kinetic-theory based rheological models to describe $N_1$ behavior using the artifice of the decomposition of $N_1$ into the kinetic and collisional contributions. They had concluded that

[15] Positive-negative-positive variations of $N_1$.

[16] This phenomenon was assumed to happen on the vorticity axis. Additionally, they had considered the fact that the arrest of the tumbling eventually occurs as the shear rate is increased.

[17] Allowing molecular orientation in the vorticity direction.

the models available were not adequate and the microstructure features (e.g., preferred distribution of collisions) should be incorporated in this theory. For this purpose, they had shown that frame-indifferent relaxation models can be used to model the $N_1$ sign variation, and according to them, the ideal choice would be the two-parameter Jeffrey's model.

More data were collected and analyzed recently by (36, 22, 90), for schizophyllan solutions, mesophase pitch, and polyvinyl chloride plastisol. The same $N_1$ sign variation behavior was verified. The latter had explained the general[18] shear rate dependent pattern follow by the steady state shear flow dividing it into three regions: (i) shear thinning at low shear rates, in this region the sample is isotropic and the growth in negative value of $N_1$ can be observed, (ii) a shear thickening region with the lyotropic system and constant viscosity with thermotropic[19] material, as soon as partial orientation starts, the negative $N_1$ reverses the trend, decreasing the negative value, and (iii) the last region is shear thinning, as the shear rate and orientation increases $N_1$ goes through zero to positive. Interestingly, (130) has developed a sliding plate rheometer to determine $N_1$, not showing the flow instabilities that limit the use of rotational rheometers in a simple shear flow. They had studied highly entangled, monodisperse polybutadiene and a commercial polystyrene. The latter material data was compared with available stressmeter data obtained by (68, 69), displaying a good agreement. Besides, the predictions provided by the Laun's empirical equation (64) were in agreement with the obtained data. They had concluded that their equipment, If the secondary flow is obviated and wall slip is taken into account, can be used to determine $N_1$ at high shear rates.

(46) had performed $N_1 - N_2$ measurements in a plate-plate geometry for a commercial shaving foam and two different repulsive emulsions composed of 80% silicone oil in water, besides wall slip was taken into account. The Money shear stress approach, previously used by (13) was shown to be applicable to the wall slip correction to $N_1 - N_2$ measurements. They had commented that "Negative normal stresses were always obtained at low shear rates because of surface curvature at the outer edge, and normal stress curves were shifted uniformly to obtain a minimum of zero" [*sic*]. However, the adopted approach was not in agreement with the literature, previously cited, which since the 70's had observed and reported the positive-negative-positive behavior of $N_1$. As a conclusion, they had calculated what they called "true yield stress" adopting the von Mises yield criterion neglecting the normal stress terms.

[18] The large difference in the molecular structure of the materials were not considered.

[19] A liquid crystal is thermotropic when exhibits of some degree of thermotropism that is a property in which the temperature gradient determines the orientation (82).

The justification given for the latter assumption was "The magnitudes of the normal stresses in shear have only a small effect on the relation between $\tau_y$ and $\sigma_y$ for the materials studied here (...)" [*sic*], where $\sigma_y$ was the yield stress that would be measured in uniform uniaxial tension and $\tau_y$ the yield stress. However intriguingly, in its results presented in its Figure 8, the contradiction can be perceived by showing that the normal stress differences order of magnitude were not negligible and can have a considerable effect on the yield stress value.

Recently, a reasonable physical explanation of the $N_1$ sign variation based on the porous nature of the polymer gels under study was given by (27). In spite of have not been as well discussed as the explanation given by (76) and extended by (62), it stills closer to engineering reality. Basically, according to them, if a polymer gel dilatates under shear $N_1$ is positive otherwise if a contraction tendency appears the material expels interstitial fluid in order to relax the pressure gradient and $N_1$ turns negative. Precisely, while the fluids and the polymer network remain viscously coupled $N_1$ is positive, by the time the fluid moves relative to the network $N_1$ becomes negative. Furthermore, they had proposed to quantitatively evaluate the $N_1$ sign variation a two-fluid model which describes a polymer gel as a biphasic system composed of a linear elastic network immersed in an incompressible viscous liquid. They had observed an excellent agreement with the data, over the considered range of oscillation frequencies, with an insensitive to frequency fitting parameters. Besides, in view of shear rheology, an unexpectedly important role of poroelastic effects involving the interstitial fluid flow of polymer gels could be observed. They had demonstrated also that, although poroelastic effects are usually assumed to affect volume-changing deformations[20], the shear response of polymer gels is highly sensitive to fluid flow and network compressibility.



## 2.4 Yielding criteria

This section will be dedicated to a brief introduction to yield criteria culminating in a simplified form famous as von Mises yielding criterion. For an anisotropic material, it can be assumed that the yielding phenomenon occurs when a combination of the components of the total stress tensor $\mathbf{T}$ reaches some critical value,

$$f(T_{11}, T_{12}, T_{13}, T_{22}, T_{23}, T_{33}) = k$$

[20]For example, compression and extension.

where $f$ is the yield function, a function that combines in a certain way the nonsymmetric components of the total stress tensor and k is some material property which can be measured experimentally. A very common alternative form for the yield function is made when the basis is changed and the stress tensor is written in terms of the principal stresses[21],

$$f(T_1, T_2, T_3, \mathbf{n}_i) = k$$

where $(T_1, T_2, T_3)$ represents the principal stresses and $\mathbf{n}_i$ the principal directions. Considering the hypothesis of isotropy, the yield function becomes independent of the principal directions $\mathbf{n}_i$, and must be a symmetric function of the principal stresses,

$$f(T_1, T_2, T_3) = k$$

The yield function can be written in terms of the three principal invariants of the stress tensor[22], because they are independent of the material orientation (51),

$$f(I_1, I_2, I_3) = 0$$

where $I_1$, $I_2$ and $I_3$ are the three principal invariants of the stress tensor. At this moment it is worth making two comments: (i) $T_i$ are the roots of $\lambda^3 - I_1\lambda^2 - I_2\lambda - I_3 = 0$, and (ii) a function of the three principal stresses is not necessarily a yield criterion, just symmetrical functions of the three principal stresses can be (51), even knowing that a function of the three invariants of the stress tensor can be expressed in terms of the principal stresses. The form of the yield function can be modified if the assumption of incompressibility is assumed. The consequence is that the plastic deformation does not cause any change in volume and, specifically, the response during the plastic regime has no influence from the spherical[23] part of the stress tensor. Furthermore, the yield function can be written in terms of the nonzero invariants[24] of the

[21] In this basis the shear stress components become zero.

[22]

$$\mathbf{I}_1 = T_1 + T_2 + T_3$$
$$\mathbf{I}_2 = T_1T_2 + T_2T_3 + T_3T_1$$
$$\mathbf{I}_3 = T_1T_2T_3$$

[23] Hydrostatic.

[24] The first invariant of the deviatoric stress $J_1$ tensor vanishes naturally, which is the trace of the deviatoric stress tensor.

deviatoric stress tensor $\boldsymbol{\sigma}$[25](48),

$$f(J_2, J_3) = 0$$

where $J_2$ and $J_3$ are the second and third invariants of the deviatoric stress tensor $\boldsymbol{\sigma}$[26]. It is important to have in mind that this theory was initally developed for metals, in which the influence of the the spherical part of the stress tensor on yielding is generally negligible (16, 17). An interesting way to visualize this abstraction is using the well known $\pi$-plane in the Haigh-Westergaard space[27] given by $T_1 + T_2 + T_3 = 0$ (see figure 2.1).

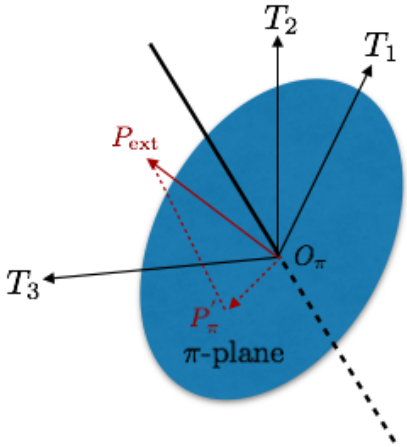


Figure 2.1: Schematic sketch of the $\pi$-plane.

Considering a point $P_{ext}(T_1, T_2, T_3)$ represented by the vector $\overrightarrow{\mathrm{O_\pi P_{ext}}}$, in the cited space, the principal deviatoric stress components can be obtained projecting $\overrightarrow{\mathrm{O_\pi P_{ext}}}$ onto the $\pi$-plane, the projection vector components are the three principal deviatoric stress components. The projection vector magnitude[28] $|\overrightarrow{\mathrm{O_\pi P'_\pi}}|$ is just $\sqrt{2J_2}$. It is worth mentioning that the second invariant of the deviatoric stress tensor ($J_2$) can be interpreted, as the distance that a generic stress state deviates from a pure hydrostatic stress state in a given Haigh-Westergaard space, i.e., it a measured of the radius of deviation from the hydrostatic state.

[25] $\boldsymbol{\sigma} = \boldsymbol{T} - \frac{1}{3}(tr\boldsymbol{T})\boldsymbol{I}$

[26] The three deviatoric stress invariants are:

$$J_1 = \sigma_1 + \sigma_2 + \sigma_3$$
$$J_2 = -(\sigma_1\sigma_2 + \sigma_2\sigma_3 + \sigma_3\sigma_1)$$
$$J_3 = \sigma_1\sigma_2\sigma_3$$

.

[27] $T_1T_2T_3$-space.

[28] Defined as the distance from $\mathrm{P_{ext}}$ to the axis $T_1 = T_2 = T_3$.

A common way in plasticity to represent the dependence of the strain, for a local state, is through the follow relation (70),

$$\varepsilon = \varepsilon(\boldsymbol{T}, \boldsymbol{\theta}, \boldsymbol{\xi}) \tag{2-1}$$

where $\varepsilon$ is the strain, $\boldsymbol{T}$ is the total stress tensor, $\theta$ the temperature and $\boldsymbol{\xi}$ is an array of what is called internal (or hidden ) variables that, roughly, represents "something else" that affects the strain. Usually, an additional equation is postulated for a body rate of sensitivity[29], for a local state, the rate of evolution of the internal variables is represented by

$$\dot{\xi}_\alpha = g_\alpha(\boldsymbol{T}, \boldsymbol{\theta}, \boldsymbol{\xi}) \tag{2-2}$$

this relation represents the rate of evolution for the internal variable $\xi_\alpha$. Applying the chain rule to 2-1,

$$\varepsilon^p_{ij} = g_{ij}(\boldsymbol{T}, \boldsymbol{\theta}, \boldsymbol{\xi}) \tag{2-3}$$

where $\varepsilon^p_{ij}$ is the plastic strain with $g_{ij} = \sum_\alpha \frac{\partial \varepsilon_{ij}}{\partial \xi_\alpha} g_\alpha$, and $g_\alpha$ is the rigth hand side of 2-2. For convenience, a relation called "viscoelastic potential" is defined $g(\boldsymbol{T}, \boldsymbol{\theta}, \boldsymbol{\xi})$, and its relation with $g_{ij}$ is given by

$$g_{ij} = \Psi \frac{\partial g}{\partial T_{ij}} \tag{2-4}$$

where $\Psi$ is a positive function, introduced by (100), that incorporates yielding characteristics of the material ($\Psi = 0$ if f$\leq 0$ else $\Psi > 0$). It is assumed that $g$ is a function of the second invariant of the deviatoric stress tensor $g(\boldsymbol{T}, \boldsymbol{\theta}, \boldsymbol{\xi}) = J_2$, applying to 2-4 we have

$$\frac{\partial J_2}{\partial T_{ij}} = (\delta_{ik}\delta_{jl} - \frac{1}{3}\delta_{ij}\delta_{kl})\sigma_{kl} = \sigma_{ij}. \tag{2-5}$$

Associating 2-3, 2-4 and 2-5

$$\varepsilon^p_{ij} = \Psi(\boldsymbol{T}, \boldsymbol{\theta}, \boldsymbol{\xi})\sigma_{ij} \tag{2-6}$$

which is known in plasticity as the "flow law". A physical consequence of this relation is that plastic deformation is volume preserving which is directly related to the fact that the energy distortion for linear, isotropic materials has the same form and it is directly proportional to $J_2$, even knowing that the energy distortion is material properties dependent being consequently not an invariant. If we take for instance the hydrostatic stress components to be zero, there is no change in volume. Therefore, the deviatoric stress tensor will not cause any change in volume because its hydrostatic components are zero. The

[29]Represents the deformation produced by a slow stressing, in general greater than that produced by a rapid stressing (see chapter one of (70)).

latter lets us conclude that the deviatoric stress cause only distortion of the material, changing just the shape but not the volume. An alternative form of the “flow rule" is

$$\varepsilon_{ij}^{p} = \dot{\lambda}\sigma_{ij}. \tag{2-7}$$

According to (70), this form was proposed by[30] Saint-Venant and others using the Tresca criterion (123) with the equation 2-6. Where $\dot{\lambda}$ is defined in terms of the yield function as

$$\dot{\lambda} = \begin{cases} \frac{1}{H} < \mathring{f} > & \text{if } f = 0 \\ 1 & \text{if } f < 0 \end{cases}$$

where $\mathring{f} = \frac{\partial f}{\partial T_{ij}}\dot{T}_{ij}$, $H = -\sum_{\alpha} \frac{\partial f}{\partial \xi_{\alpha}} \frac{g_{\alpha}}{\Psi}$ and we are using here the Macauley bracket notation $< x > = xh(x)$ where $h(x)$ is the heaviside function. At this point, a special yield function can be defined as follows,

$$f(\boldsymbol{T}, \boldsymbol{\xi}) = \sqrt{J_2} - K(\boldsymbol{\xi}) = 0 \tag{2-8}$$

where $K(\boldsymbol{\xi})$ is the yield stress in simple shear at the current value of $\boldsymbol{\xi}$. This yield function in connection with the “flow rule" 2-7 represents what is known as the von Mises criterion (work published in (87)). In his work, von Mises derived the general equations for plasticity, accompanied by his well-known pressure-insensitive yield criterion (stated in (48)). This yield criterion suggests that yielding starts when the intensity of the second deviatoric stress invariant reaches some critical value. Another way to interpret this criterion, common in material science is using a scalar quantity called von Mises stress $\sigma_v$ defined as

$$\sigma_v = \sqrt{3|J_2|} \tag{2-9}$$

where the $J_2$ is the previous commented second deviator invariant which can be expressed as

$$J_2 = \frac{1}{2}\left[\mathrm{tr}(\boldsymbol{\sigma}^{\mathbf{2}}) - \frac{1}{3}(\mathrm{tr}\boldsymbol{\sigma})^2\right] \tag{2-10}$$

Thus, the von Mises stress can be represented by

$$\sigma_v = \sqrt{\frac{1}{2}\mathrm{tr}(\boldsymbol{\sigma}^2)} \tag{2-11}$$

this criterion assumes that yielding begins when the von Mises stress reaches certain critical value, known as the yield strength (or, more commonly in Rheology, yield stress) $\sigma_y$, which is defined as a scalar material property defined as the level of stress required in which bellow no irreversible flow occurs.

[30]First proposed by Lévi (see chapter 3 of (70)).

# 3
# PART I - The importance of the contribution of the normal stresses

This chapter is dedicated to the first part of the present research which consists basically in evaluating properly the apparent yield stress of eight elasto-viscoplastic materials, pastes and gels. For this purpose, a sequence o standard constant shear stress tests were performed for each material, estimating the critical stress ($\sigma_{21}$) which represents the mean value obtained between the stress values of the curves in which the material flows[1] and does not flow with an accurate tolerance[2]. After that, a proposed test to evaluate the proper values of the normal stress differences was performed for each material, giving the value of $N_1 - N_2$ at the critical stress value ($\sigma_{21}$) previously obtained. Following, with those results the intensity of the second invariant of the deviatoric stress tensor was evaluated for two cases considering and neglecting $N_1$ and $N_2$ for each material. Lastly, the importance of taking into account the normal stress differences in order to estimate properly the apparent yield stress in shear flow is discussed.

The materials chosen for experimental evaluation are Carbopol® 0.5%, Carbopol® 1.0%, commercial hair gel A[3], commercial hair gel B[4], commercial hair gel C[5], commercial grease lubrication[6], commercial solder paste[7] and, commercial putty[8]. This choice is justified by the following reasons: (i) Carbopol® is one of the favorite choices for rheological experiments in view of its capacity of reproducing a vast range of shear thinning behaviors, (ii) commercial materials were chosen because of its manufacture and repeatability control, and (iii) different pastes were chosen to show that it is possible to reached static equilibrium for materials with other microstructure characteristics, compared to the gels cited.

[1]By the time the strain rate starts to increase it indicates that the material is starting to deform.
[2]Related to the small difference in Pa of the considered stresses.
[3]Product name “Bozzano 2 fixação média", brand Bozzano.
[4]Product name “Bozzano 3 forte fixação", brand Bozzano.
[5]Product name “Bozzano 4 mega forte fixação", brand Bozzano.
[6]Brand Lacxe.
[7]Brand Emavi.
[8]Brand Lacxe.

It is important to mention the Carbopol® preparation procedure. A mechanical agitator with a helical shovel is added to a metal container filled with a proper amount of deionized water and set at 1200 rpm. After that, proceed to add the Carbopol®, previously combed, preferably weigh in a low glass container, and slowly pour, let the solid fall on the side of the pot, being careful not letting solid particles stand on the shove. Let it mix for 15 minutes then turn off the agitator for 30 minutes and change the helical blade by the anchor blade. Lastly, weigh the NaOH in analytical balance and plastic beaker, turn on the mixer using the 300 rpm, add the NaOH very slowly from the side of the bucket and, left to stir for 7 days. If a large amount of Carbopol® is prepared, more than 5 kg, after 7 days there is a need to mix with the helical paddle for another hour to remove bubbles.

## 3.1 Constant shear stress tests

The constant shear stress tests (or, more commonly, creep tests) consists of imposing a constant stress in a sample recording the shear rate response over time with a view, usually, to determine the yield stress ( a concept well defined in (29)). In the case of yield stress materials, experimentally, if the imposed tension magnitude is below the value of the yield stress, the data shows that the strain will tend to a constant value and then the strain rate will tend to zero, indicating that there is no flow. By the time the strain rate starts to increase it indicates that the material is starting to deform. It is important to emphasize that the experiments of this section will be used to estimate the critical stresses in a simple shear flow ($\sigma_{21,y}$) for each material considered, it is not correct to call those values yield stresses without a proper investigation on normal stresses. Each critical stress was estimated by taking the mean value obtained between the stress values of the curves in which the material flows and does not flow. The following experimental procedure was adopted for each experiment using a rotational shear stress controlled rheometer[9]: (i) fit the cross-hatched plates[10] in the rheometer[11], (ii) set and calibrate the initial gap and other parameters, (iii) with a glass syringe: withdraw the sample from the commercial container, place the material in the center of the bottom plate of the rheometer, eliminate air bubbles pulling it out of the sample one at a time.

Several creep tests were performed for each material in order to estimate the critical stresses in simple shear flow, the test was performed for 2 hours

[9] Haake Mars III.

[10] Whose diameter is 60 mm.

[11] For the putty a smooth plates with 35 mm of diameter were used because the rheometer maximum normal force was exceeded when a cross-hatched plates were employed.

with a gap of 1 mm, and a special chamber was used to avoid evaporation stabilize the temperature and a preset 300s thermostating time was used. The results are shown in Figures 3.1, 3.2, 3.3, 3.4, 3.5, 3.6, 3.7, and 3.8. Besides, the critical yield stress values estimated for each material are shown in the table 3.1.

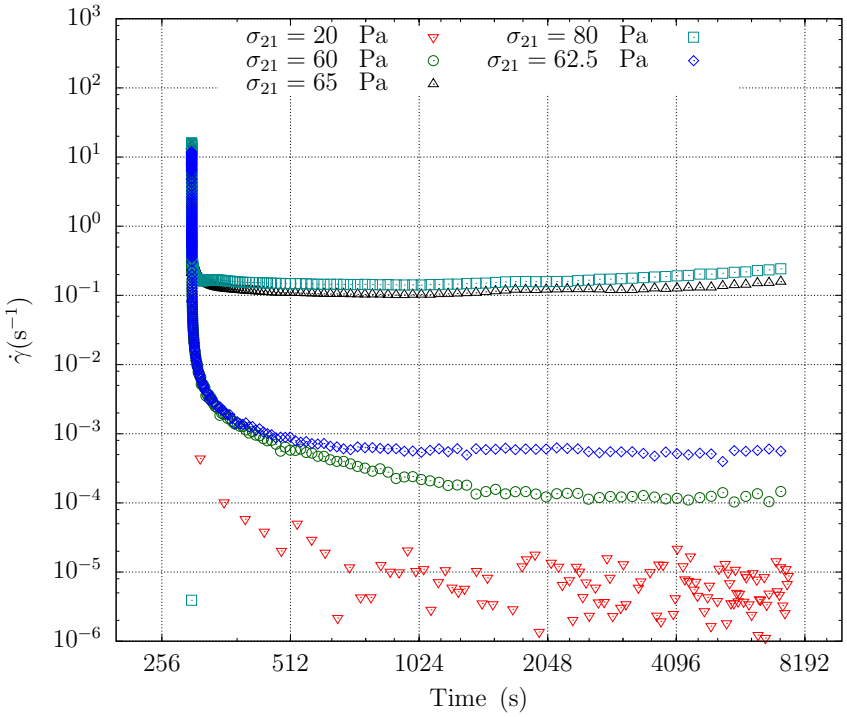


Figure 3.1: Constant shear stress tests for the Carbopol® 0.5%, using cross-hatched plates with an initial gap of 1 mm during 7200s.

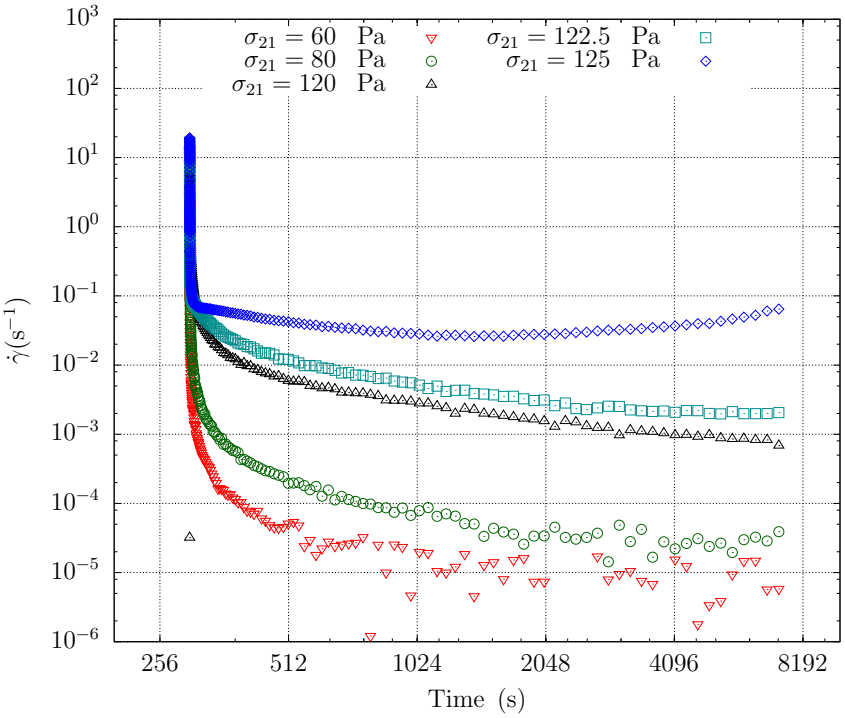


Figure 3.2: Constant shear stress tests for the Carbopol® 1.0%, using cross-hatched plates with an initial gap of 1 mm during 7200s.

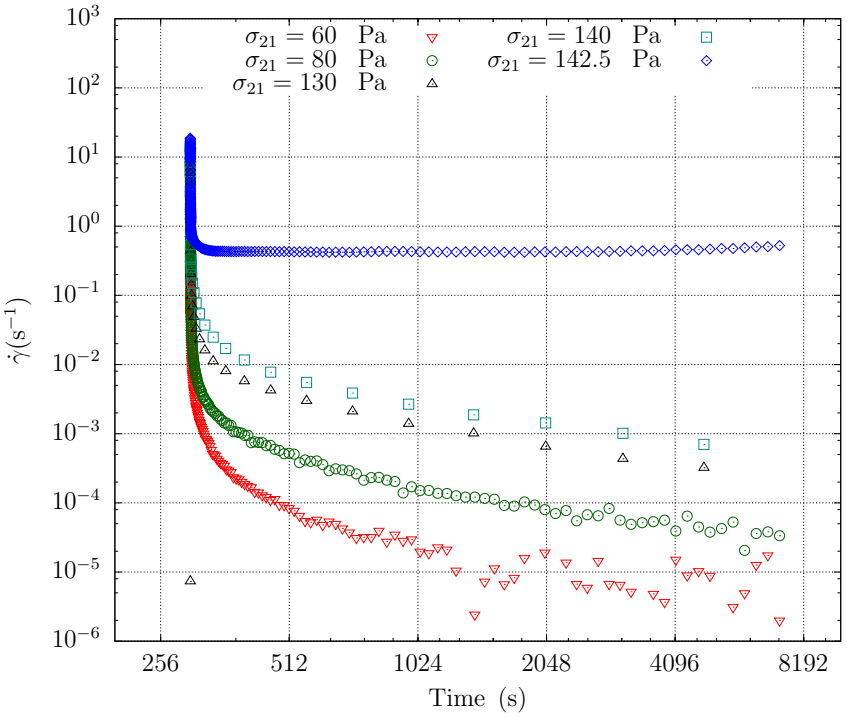


Figure 3.3: Constant shear stress tests for the comercial hair gel A, using cross-hatched plates with an initial gap of 1 mm during 7200s.

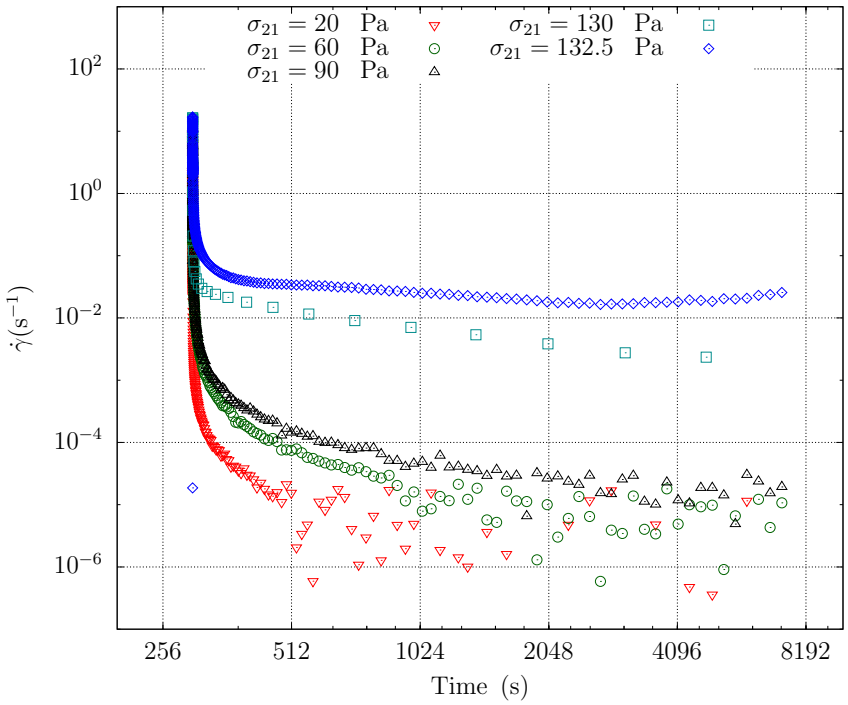


Figure 3.4: Constant shear stress tests for the comercial hair gel B, using cross-hatched plates with an initial gap of 1 mm during 7200s.

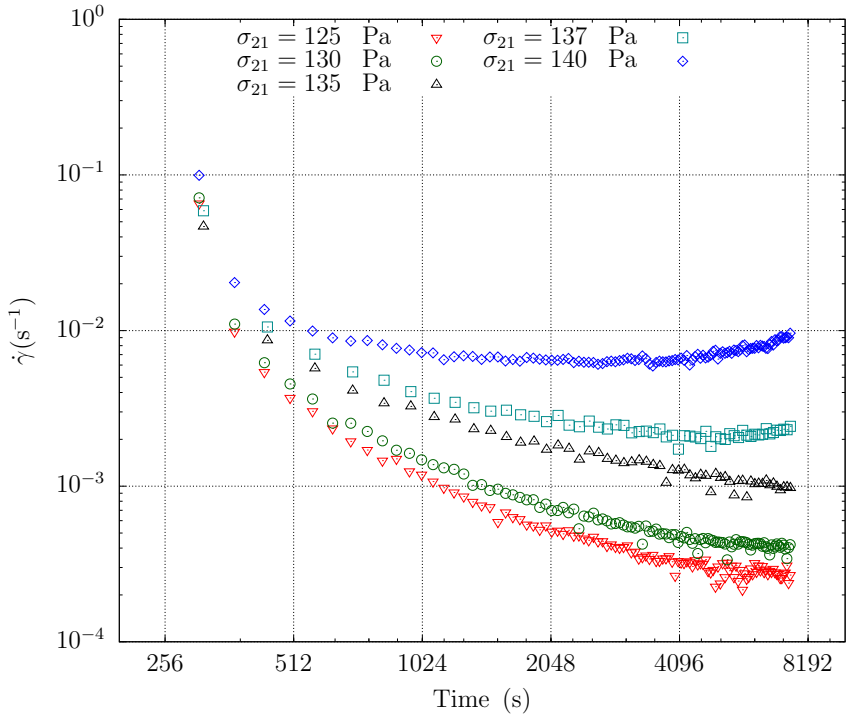


Figure 3.5: Constant shear stress tests for the comercial hair gel C, using cross-hatched plates with an initial gap of 1 mm during 7200s.

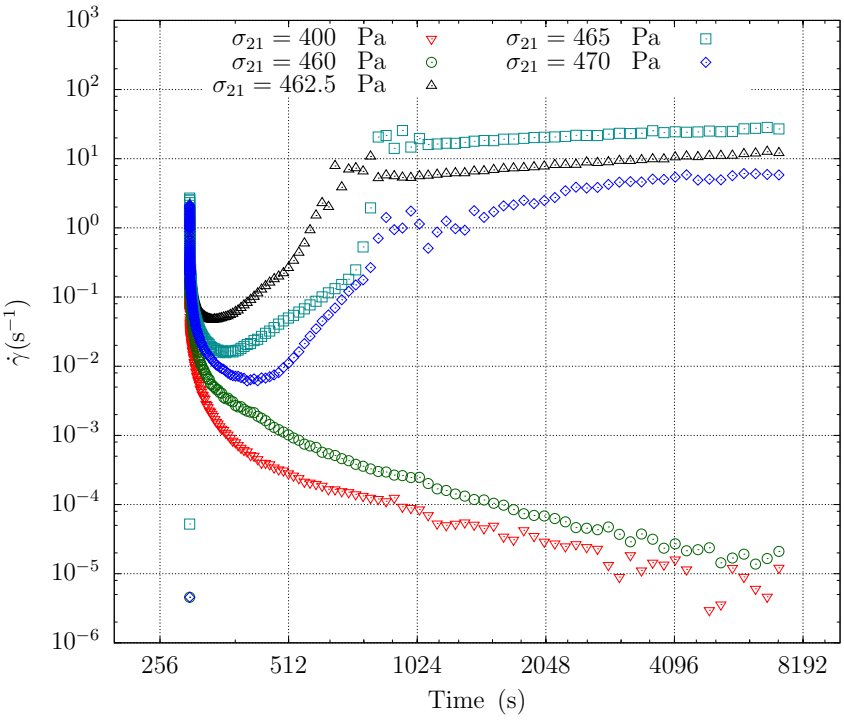


Figure 3.6: Constant shear stress tests for grease lubrication, using cross-hatched plates with an initial gap of 1 mm during 7200s.

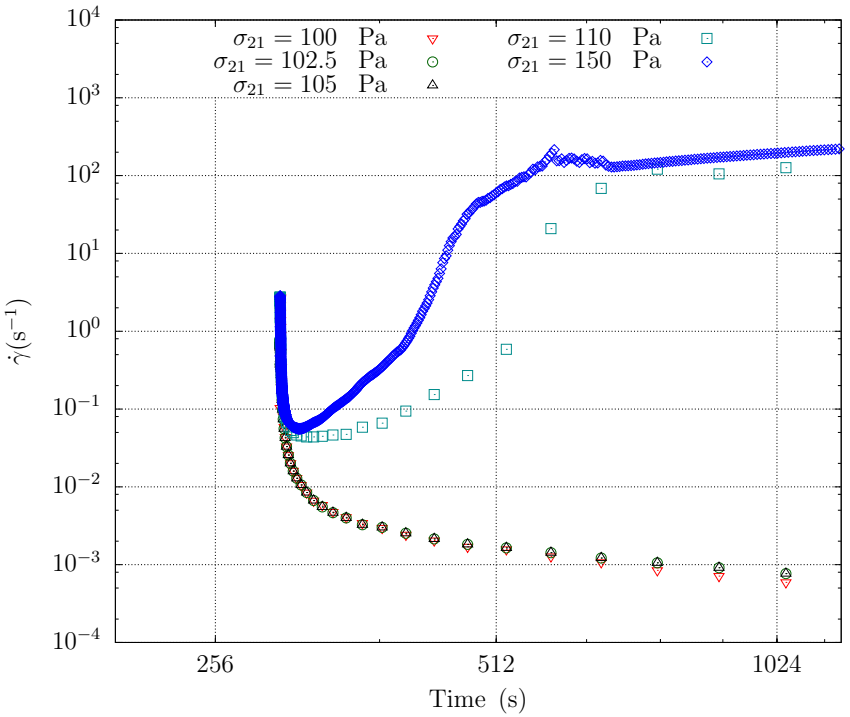


Figure 3.7: Constant shear stress tests for solder paste, using cross-hatched plates with an initial gap of 1 mm during 7200s.

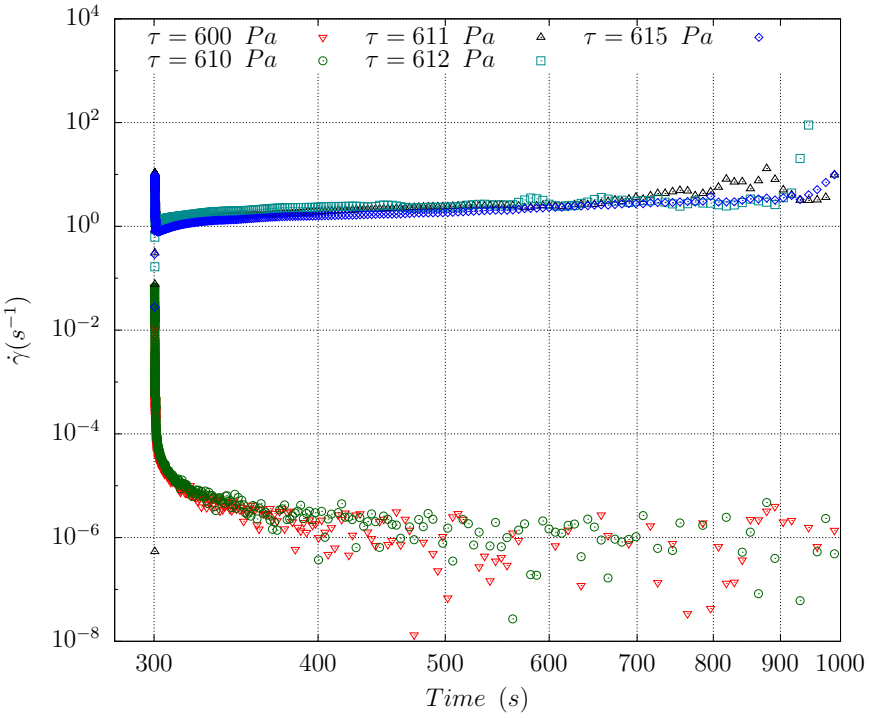


Figure 3.8: Constant shear stress tests for putty, using smooth plates with 35 mm of diameter and an initial gap of 1.5 mm during 7200s.

Table 3.1: In this table, we show for each material analyzed in this work the critical stresses estimated.

| Materials | $\sigma_{21,y}$ (Pa) |
|---|---|
| Carbopol® 0.5% | 61.5 |
| Carbopol® 1.0% | 121.5 |
| Comercial hair gel A | 141.25 |
| Comercial hair gel B | 131.25 |
| Comercial hair gel C | 136.0 |
| Grease lubrication | 461.5 |
| Solder paste | 105 |
| Putty | 610.5 |
| **Constant shear stress** | |
| Initial gap $(mm)$ | 1 |
| Cross hatched plates diameter$(mm)$ | 60 |

For simplicity, in order to comment the behavior displayed by the materials analyzed, we will adopt the following nomenclature[12]: smooth (commercial gel C), standard (Carbopol® 0.5%, Carbopol® 1% and commercial gels A and B) and hard (grease, solder paste, and putty). For the smooth materials, a very slow decrease tending to the zero shear rate could be observed, below

[12]This classification is related to this section.

the critical stress, probably due to the characteristic time adopt in this experiment. For values above the critical stress, a slight and gradual increase in shear rate was noticed. The standard materials have shown the expected viscosity bifurcation behavior. Below the critical stress, the curves declined to the zero shear rate and above this value, a jump in shear rate could be observed followed by a gradually rise. Lastly, the hard materials have shown a sudden drop to zero shear rate, for stress levels below the critical stress, and for values above a dramatic increase in shear rate was observed. In the latter materials, there were different behaviors for stress levels above the critical level. For the putty, after a critical jump in shear rate a dramatic drop and then a gradual increase followed. For the grease and solder paste displayed after the jump in shear rate, a smooth decrease, and transition to a linear monotonic increasing profile followed by another transition to a gradual increase tendency.

## 3.2 Normal stress differences measurements

This section is dedicated to a description of the experiments performed in order to estimate the critical values of $N_1$ and $N_2$ for each material. The latter was defined as the values which correspond to the critical stress levels ($\sigma_{21}^c$), previously obtained in the last section, for each material. It was used a hybrid rheometer[13] and two geometries the cross-hatched plates and the sandblasted cone and plate both with 60 mm of diameter [14]. The initial gap between plates was 1 mm[15] and for the latter, a truncation gap of 29 $\mu$m with an angle of 1.009° was employed[16]. The reason why it was chosen two different geometries to perform the same experimental procedure, was the determination of the second normal stress difference $N_2$, which will be explained later. The experiment consists of the following steps: (I) calibrate, and set the material properly and adopting similar sample preparation procedures as in the last section, (ii) let the material rest for 2 hours with a special chamber in order to avoid evaporation, (iii) let the temperature stabilize for 20 minutes until no longer temperature gradient can be observed, (iv) let the sample experienced a pre-shear stress loading of $10^{-3}$ Pa for 20 minutes and, (v) apply a shear stress ramp recording $N_1 - N_2$ or $N_1$ which will be explained as follows.

[13]Discovery HR-3 hybrid rheometer.

[14]Except for the putty in which a 40 mm of diameter smooth parallel plates and cone and plate geometries were used, due to the material consistency which causes an exceedance of the initial normal force supported by the rheometer settings.

[15]Except for the putty in which an initial gap of 2.144 mm was adopted.

[16]Except for the putty in which a truncation gap of 52 $\mu$m with an angle of 2.011° was employed.

For a steady isothermal shearing flow, considering the cone and plate geometry, assuming that the free liquid surface is spherical, the cone angle very small and the liquid inertia, surface tension, and edge effects are negligible. It can be shown that the first normal stress difference, for rheometrical measurement purposes, can be calculated by ((55), example 10.2-1 of (14), and page 209 of (72)),

$$N_1 = \frac{2F}{\pi R^2} \tag{3-1}$$

where $T$ is the torque, $R$ the plate radius and $F$ the vertical force. Additionally, for the same flow, if a parallel plate geometry is chosen considering that the free liquid surface is cylindrical and neglecting the liquid inertia, surface tension, and edge effects. A different measurement can be done in which the difference $N_1 - N_2$ can be estimated by the following relation ((59, 55), example 10.2-2 of (14), and page 222 of (72)),

$$(N_1 - N_2)_{\dot{\gamma}_R} = \frac{2F}{\pi R^2}\left(1 + \frac{1}{2}\frac{\ln F}{\ln \dot{\gamma}_R}\right) \tag{3-2}$$

where $\dot{\gamma}_R$ is the apparent shear rate calculated at the measured gap and $(N_1 - N_2)_{\dot{\gamma}_R}$ is the difference $N_1 - N_2$ at the correspoding $\dot{\gamma}_R$. Therefore, using the results obtained by the equations 3-1 and 3-2 for each material, we can estimate the corresponding values of $N_2$. The values obtained for each material are presented at Table 3.2, and the data from each test and material can be seen at the Figures 3.9(a), 3.9(b), 3.10(a), 3.10(b), 3.11(a), 3.11(b), 3.12(a), 3.12(b), 3.13(a), 3.13(b), 3.14(a), 3.14(b), 3.15(a), 3.15(b), 3.16(a), 3.16(b).

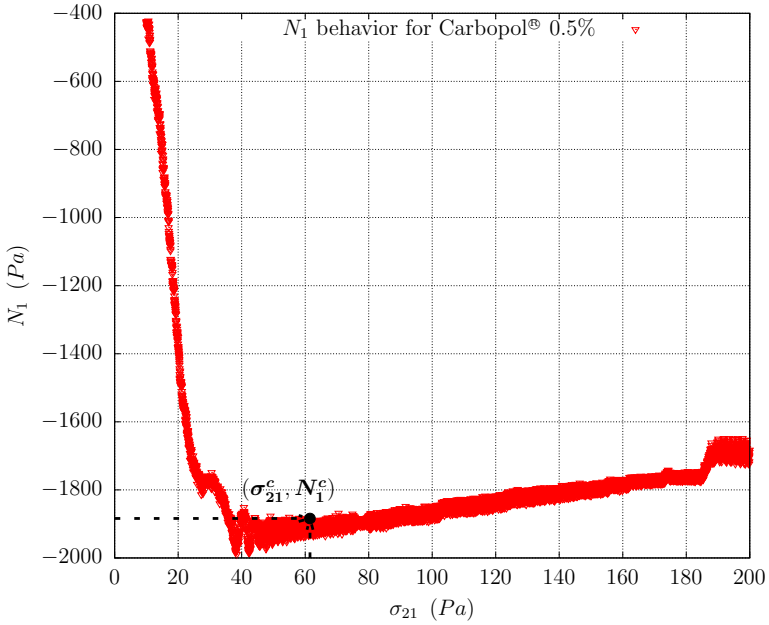


(3.9(a)) Sandblasted cone and plate.

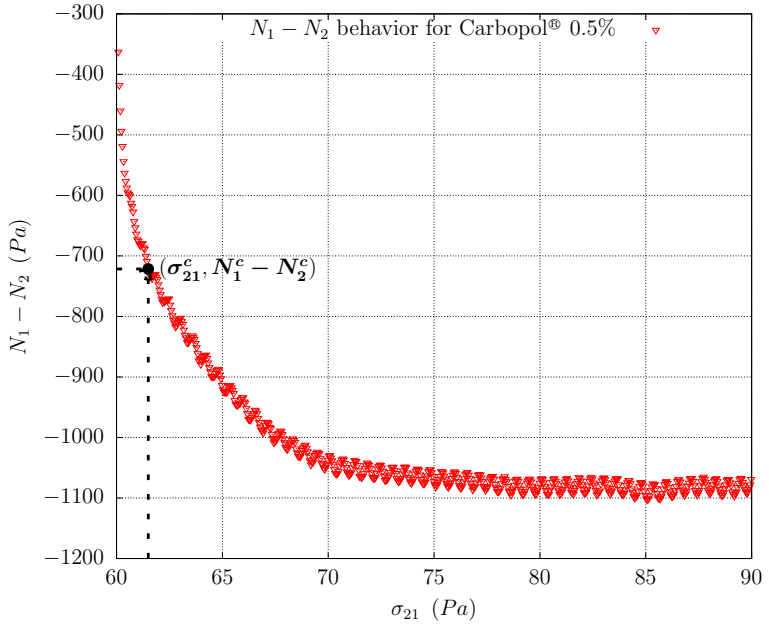


(3.9(b)) Parallel cross-hatched plates.

Figure 3.9: Stress ramp test for the Carbopol® 0.5%.

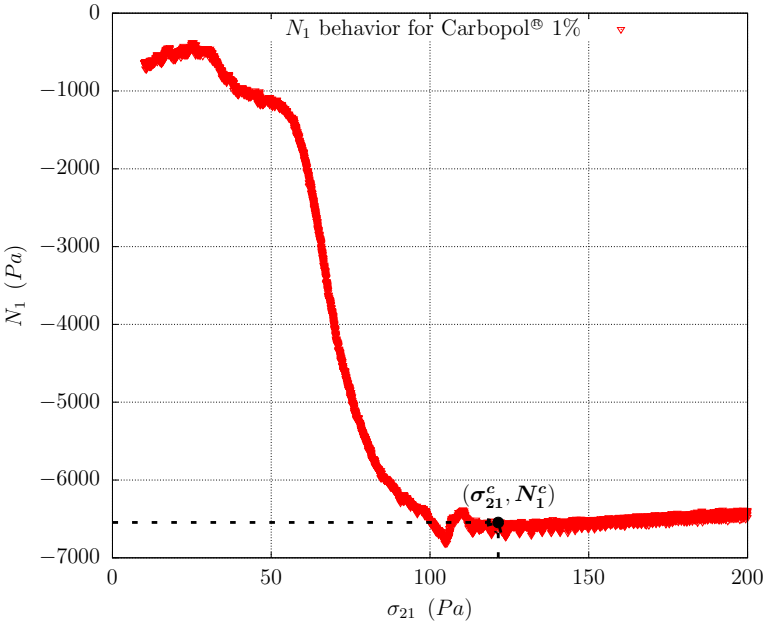


(3.10(a)) Sandblasted cone and plate.

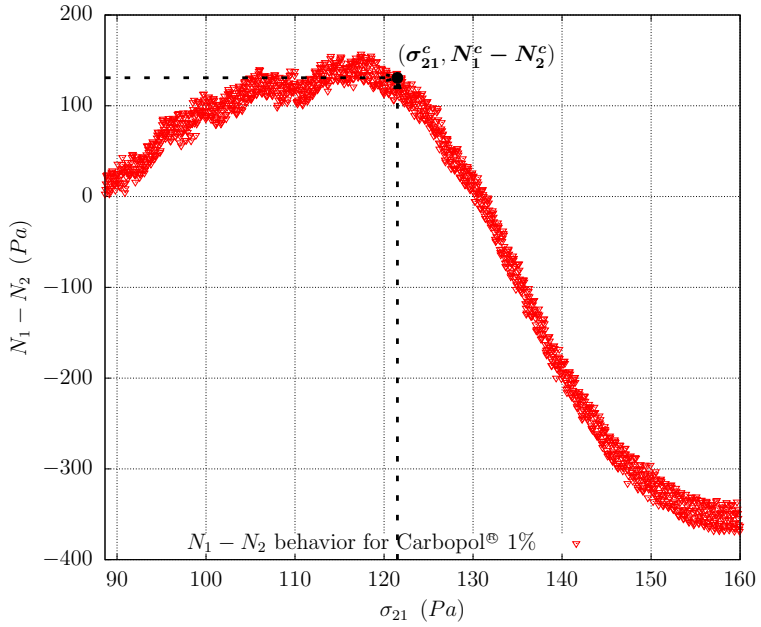


(3.10(b)) Parallel cross-hatched plates.

Figure 3.10: Stress ramp test for the Carbopol® 1%.

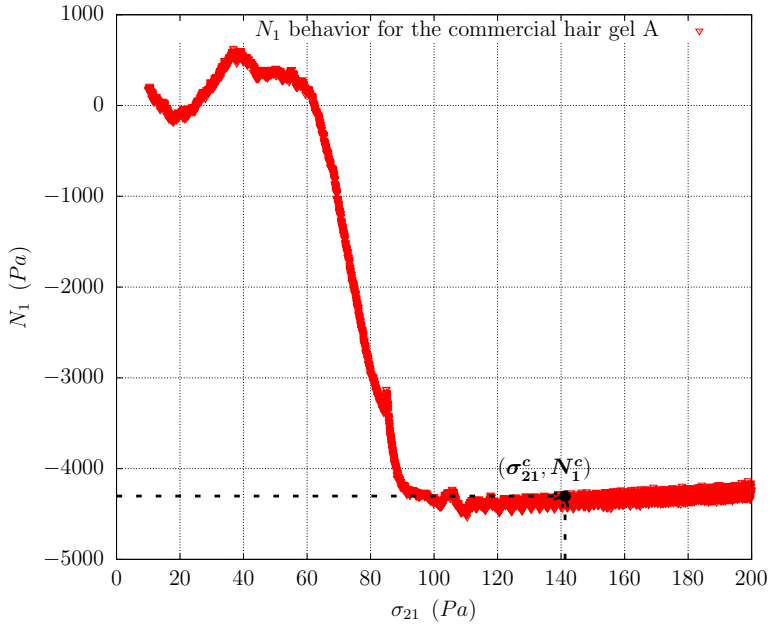


(3.11(a)) Sandblasted cone and plate.

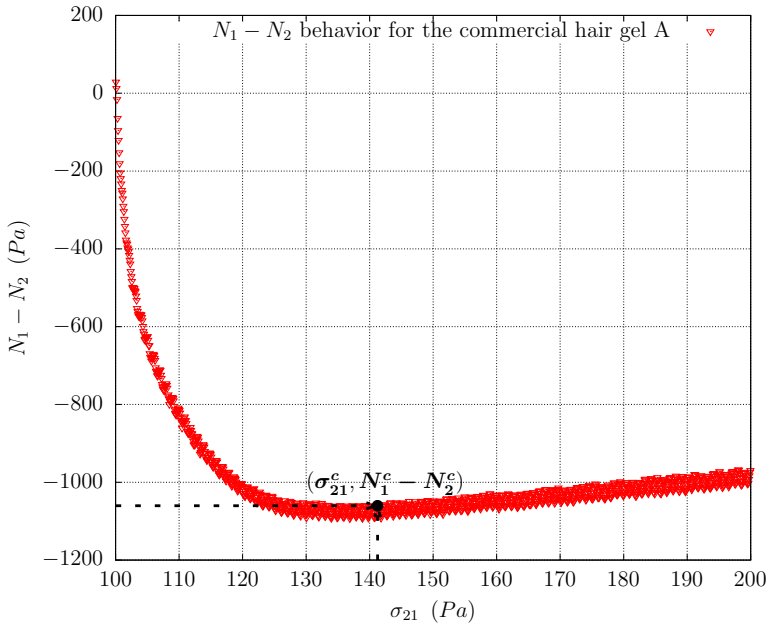


(3.11(b)) Parallel cross-hatched plates.

Figure 3.11: Stress ramp test for the comercial hair gel A.

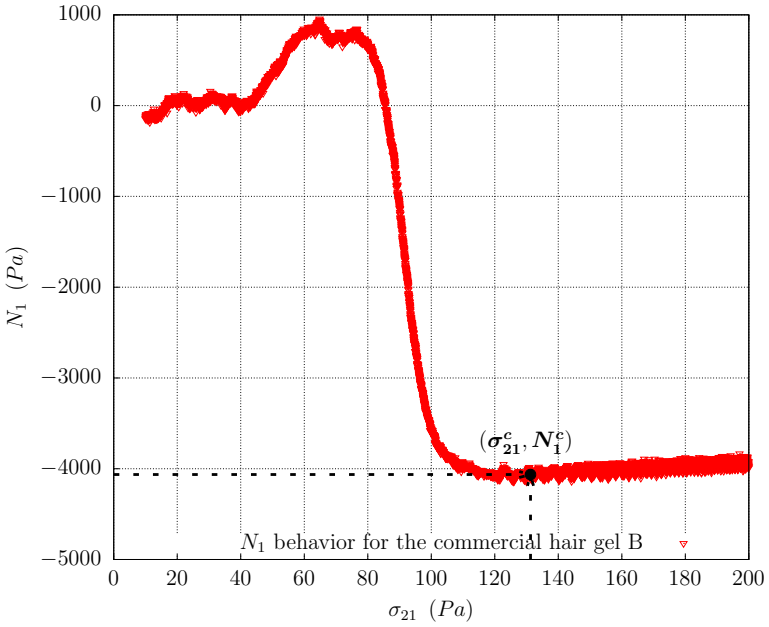


(3.12(a)) Sandblasted cone and plate.

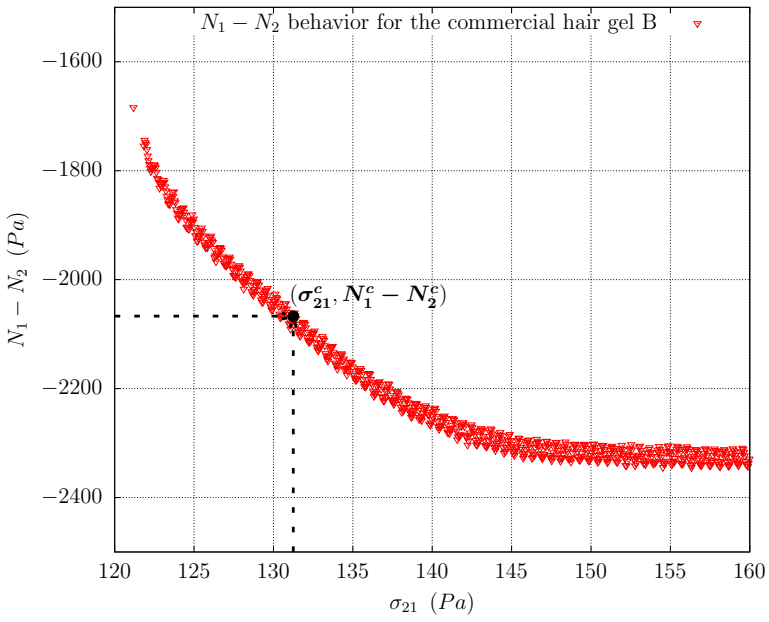


(3.12(b)) Parallel cross-hatched plates.

Figure 3.12: Stress ramp test for the comercial hair gel B.

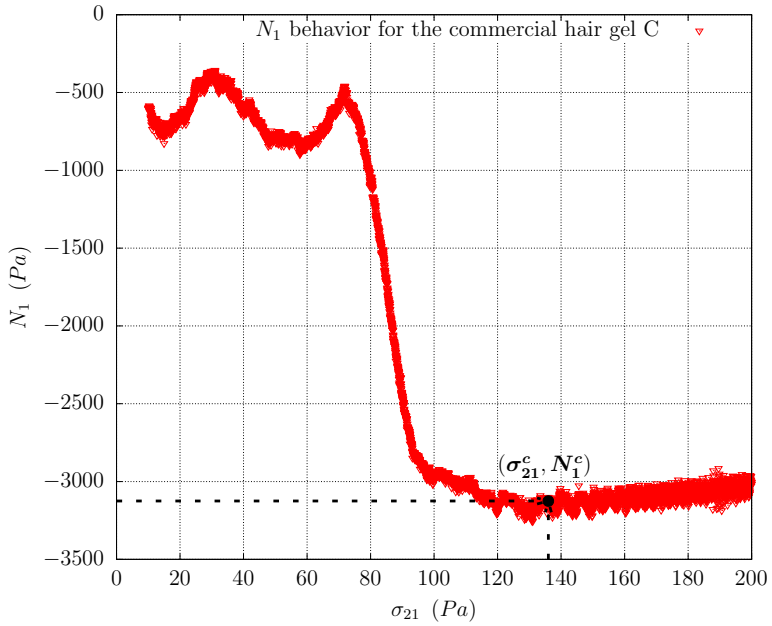


(3.13(a)) Sandblasted cone and plate.

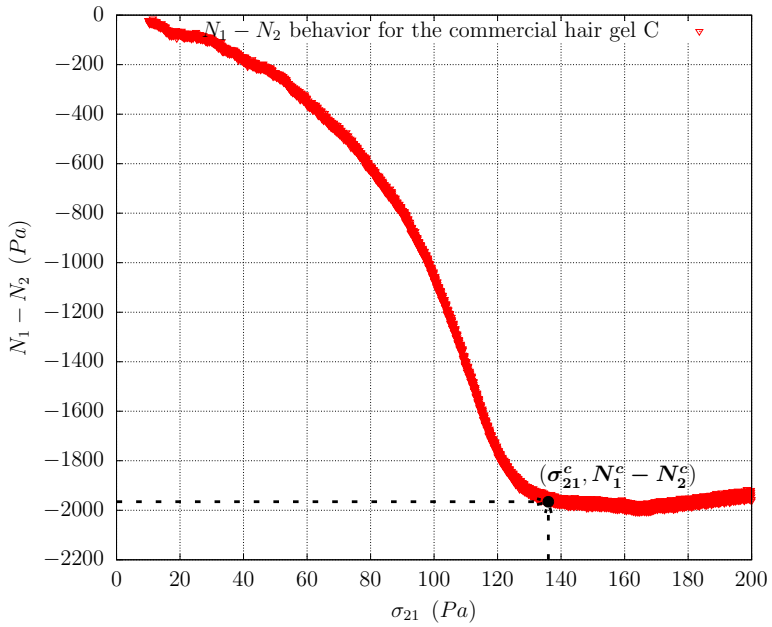


(3.13(b)) Parallel cross-hatched plates.

Figure 3.13: Stress ramp test for the comercial hair gel C.

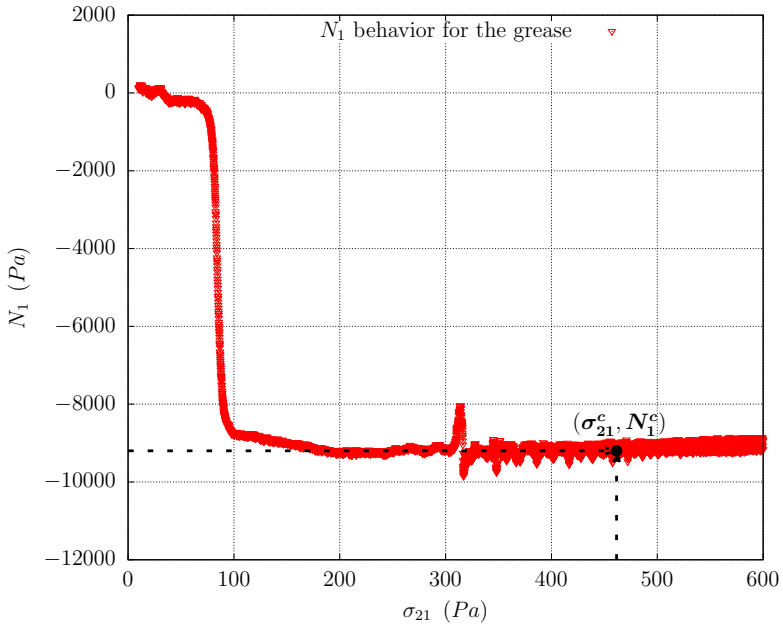


(3.14(a)) Sandblasted cone and plate.

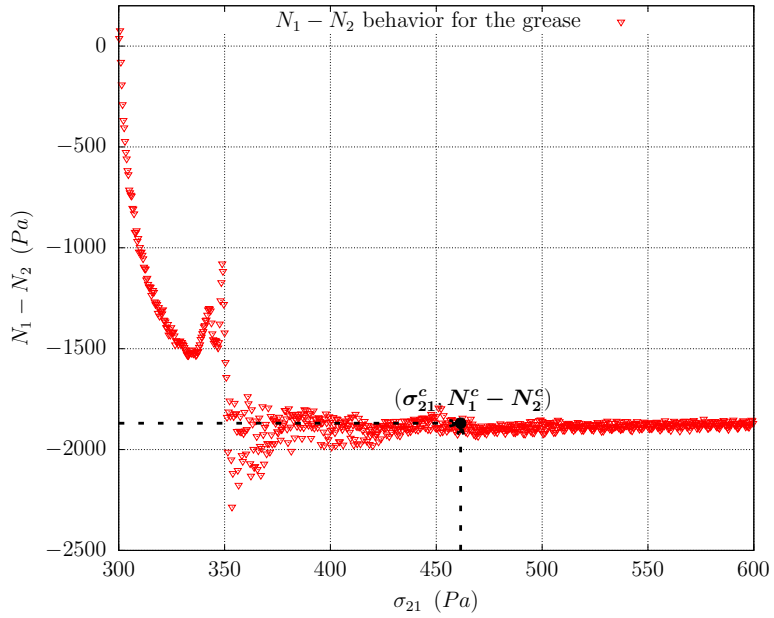


(3.14(b)) Parallel cross-hatched plates.

Figure 3.14: Stress ramp test for the grease lubrication.

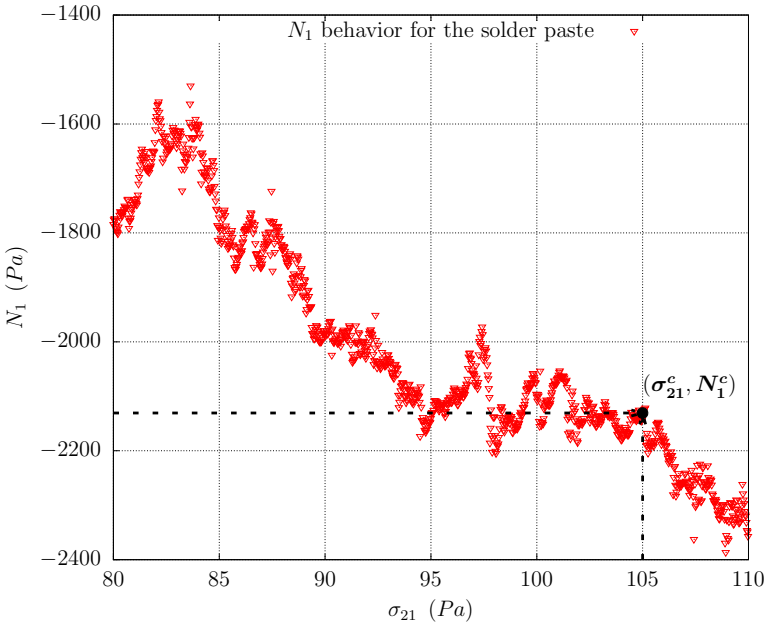


(3.15(a)) Sandblasted cone and plate.

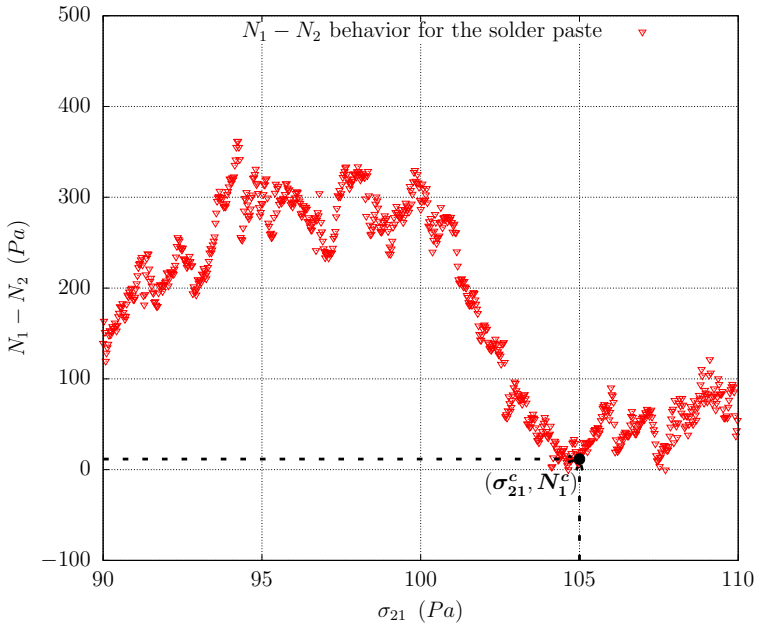


(3.15(b)) Parallel cross-hatched plates.

Figure 3.15: Stress ramp test for the solder paste.

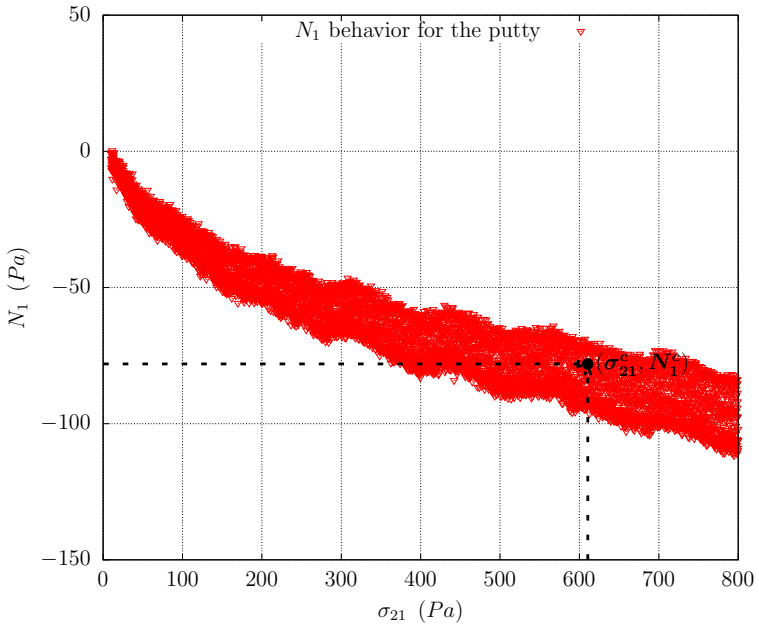


(3.16(a)) Smooth cone and plate.

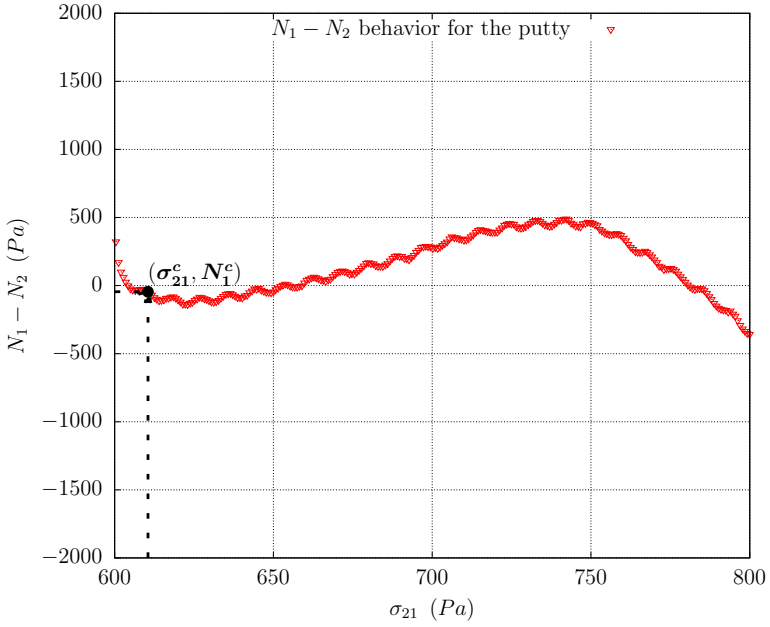


(3.16(b)) Smooth parallel plates.

Figure 3.16: Stress ramp test for the putty.

Table 3.2: In this table, we show for each material analyzed in this work the critical values of $N_1$ and $N_2$ measured at the critical stresses ($\sigma_{21}^c$) level previously obtained at section 3.1.

| Materials | $(N_1 - N_2)^c$ (Pa) | $N_1^c$ (Pa) | $N_2^c$ (Pa) |
|---|---|---|---|
| Carbopol® 0.5% | -721.53 | -1884.09 | -1162.56 |
| Carbopol® 1.0% | 130.88 | -6545.28 | -6676.16 |
| Comercial hair gel A | -1060.27 | -4302.82 | -3242.55 |
| Comercial hair gel B | -2066.97 | -4064.10 | -1997.13 |
| Comercial hair gel C | -1965.46 | -3124.70 | -1159.24 |
| Grease lubrication | -1869.70 | -9199.61 | -7329.91 |
| Solder paste | 11.56 | -2130.71 | -2142.27 |
| Putty | -45.25 | -78.08 | -32.83 |
| **Shear stress ramp - normal stress measurements** | | | |
| $N_1$ - cone and plate | | | |
| $N_1 - N_2$ - parallel cross-hatched plates | | | |

It could be observed for all materials studied, partially or completely, the general shear rate dependent $N_1$ sign variation pattern in agreement with (56, 57, 66, 36, 22, 90) (see section 2.3 for further details). Displaying positive values of $N_1$ at small shear stresses, consequently at small shear rates[17]. Besides, at intermediate values of shear stresses, all the materials have shown negative values of $N_1$. Lastly, at high shear rates, an increasing tendency of $N_1$ rose[18].

Now we will discuss in detail the profiles of $N_1$ and $N_1 - N_2$ found in our experiments for each material analyzed, using the physical explanation for the signal variation given by (27). Based on the direct measurements of $N_1$ using cone and plate geometry, five materials[19] have shown a quite similar behavior in which the $N_1$ profiles had initially raised indicating a dilating tendency of the sample followed by a transition to a linear monotonic decreasing indicating that the sample is contracting with a transition to an apparent constant negative plateau indicating that the material can no longer contract. It worth to mention the peculiar differences among these materials: (a) Carbopol® 1% at the beginning had negative values of $N_1$ which means the initial rise was the microstructure trying to recover (see Figure 3.10(a)), (b) Commercial hair gels A and B, had in fact dilated initially showing positive values of $N_1$ (see Figures 3.11(a) and 3.12(a)), (c) The grease had also dilated at the beginning but with lower absolute values comparing to the previous commented materials followed

[17]Excepted by the Carbopol® 0.5%, Carbopol® 1%, commercial hair gel C and solder paste.

[18]Excepted by the solder paste and putty.

[19]Carbopol® 1%, grease, and commercial hair gels A, B and C

by a dramatic drop, showing a critical contract behavior going almost directly to the negative plateau (see Figure 3.14(a)), and (d) Commercial hair gel C had shown initially an oscillatory behavior in which contraction followed by a dilating microstructure recovery until the material can no longer resist and start to continuously contract with a linear monotonic decreasing profile until a transition to a negative plateau (see Figure 3.13(a)).

In another hand, a peculiar behavior was presented by Carbopol® 0.5%, solder paste, and putty. The carbopol® 0.5% has shown a dramatic linear drop indicating a critical sample contraction with a transition to a linear monotonic increasing profile indicating a dilating microstructure recovery (see Figure 3.9(a)). The solder paste presented a sawtooth profile in which an oscillatory behavior took place with a continuously decreasing profile indicating that the material was contracting continuously (see Figure 3.15(a)). Lastly, the putty which was an extremely difficult experiment to perform due to the material consistency has shown an average continuous decrease, indicating that the sample was contracting. It is important to mention that this contraction was very slow which can be observed by its absolute values (see Figure 3.16(a)).

Turning our attention to $N_1 - N_2$ direct measurements using cross-hatched parallel plates. The materials have shown a very different N1-N2 profile behavior described as follows: [Behavior I] (a) Carbopol® 0.5% and the commercial hair gels B and C had displayed a very behaved profile in which a monotonically decrease took place with a smooth transition to an apparent constant negative plateau indicating that the material can no longer contract (Figures 3.9(b), 3.12(b), and 3.13(b)), it is worth to mention that in the case of the commercial hair gel C the monotonically decrease was a concave profile, (b) Interestingly, the grease, showed the same behavior except for the fact that it presented a disturbance during the transition to the negative constant plateau (Figure 3.14(b)), (c) A similarly behavior was presented also by the commercial hair gel A, except by the fact that after the monotonically decrease instead of a plateau as in the previously commented materials, a dilating tendency showed up with a linear increase (Figure 3.11(b)), [Behavior II] Carbopol® 1% initially had risen indicating that the sample was dilating after reaching a bottom followed by decrease indicating microstructure recovering then a linear decline showing that the contraction phenomenon have being predominant until an apparent change in slope (Figure 3.10(b)), [Behavior III] The solder paste has shown initially a similar behavior then the previous material, an initially monotonically increase indicating that the sample was dilating after reaching a bottom followed by decrease indicating microstructure recovering, but instead of keeping contracting after reach a zero plateau he displayed an

oscillatory dilating behavior in which the material oscillates in between zero and positive $N_1 - N_2$ values (Figure 3.15(b)), and [Behavior IV] The putty presented a sawtooth profile in which an oscillatory behavior took place with an initial contraction followed by a recovery dilatancy of the microstructure then successively (Figure 3.16(b)).

## 3.3 Yield stress evaluation and discussion

This section will be dedicated to discussing the importance in consider the normal stress differences to determine the apparent yield stresses of elasto-viscoplastic materials. It is a common procedure on the scientific community to consider the apparent yield stress as the estimated critical stress obtained on the flow curve or more accurate by a sequence of constant shear stress tests. By assuming these values, we are considering that the components of the intensity of the second invariant of the deviatoric stress tensor are negligible. In the present analysis, using the previously obtained data for $N_1$ and $N_2$, we are going to calculate the yield strength and compare it with the values of the critical stresses $\sigma_{21}^c$ previous obtained, commonly adopted as the apparent yield stress.

Considering simple shear flow (see figure 3.17) the deviatoric stress is represented by

$$\boldsymbol{\sigma} = \begin{bmatrix} \sigma_{11} & \sigma_{12} & 0 \\ \sigma_{21} & \sigma_{22} & 0 \\ 0 & 0 & \sigma_{33} \end{bmatrix}.$$

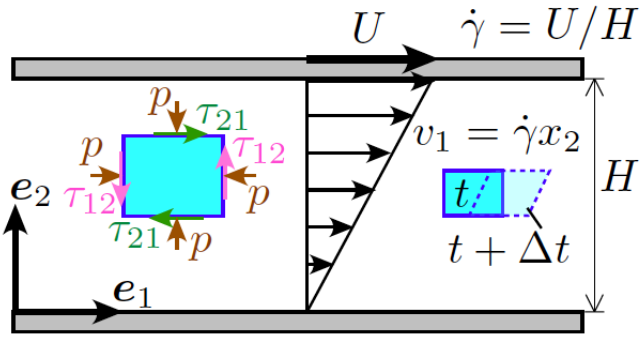


Figure 3.17: Simple shear flow.

By definition we have,

$$\left.\begin{aligned} \mathrm{tr}(\sigma) = \sigma_{11} + \sigma_{22} + \sigma_{33} = 0 \\ \sigma_{11} - \sigma_{22} = N_1 \\ \sigma_{22} - \sigma_{33} = N_2 \end{aligned}\right\} \quad \Longrightarrow \quad \begin{cases} \sigma_{11} = \dfrac{1}{3}(2N_1 + N_2) \\ \sigma_{22} = -\dfrac{1}{3}(N_1 - N_2) \\ \sigma_{33} = -\dfrac{1}{3}(N_1 + 2N_2) \end{cases}$$

Writing the deviator tensor in terms of measurable quantities $(\sigma_{21}, N_1, N2)$,

$$\boldsymbol{\sigma} = \begin{bmatrix} \frac{1}{3}(2N_1 + N_2) & \sigma_{21} & 0 \\ \sigma_{21} & -\frac{1}{3}(N_1 - N_2) & 0 \\ 0 & 0 & -\frac{1}{3}(N_1 + 2N_2) \end{bmatrix}$$

Thus,

$$\boldsymbol{\sigma}^2 = \begin{bmatrix} \frac{1}{9}(2N_1 + N_2)^2 + \sigma_{21}^2 & \frac{\sigma_{21}}{3}(N_1 + 2N_2) & 0 \\ \frac{\sigma_{21}}{3}(N_1 + 2N_2) & \sigma_{21}^2 + \frac{1}{9}(N_1 - N_2)^2 & 0 \\ 0 & 0 & \frac{1}{9}(N_1 + 2N_2)^2 \end{bmatrix}$$

Therefore, the von Mises stress can be calculated as follows

$$\sigma_v = \sqrt{\frac{1}{2}(\mathrm{tr}\boldsymbol{\sigma})^2} = \sqrt{\sigma_{21}^2 + \frac{1}{3}(N_1^2 + N_1 N_2 + N_2^2)} \tag{3-3}$$

and thus the yield stress $\sigma_y$, using equation 2-11, in simple shear flow is given by

$$\sigma_{\mathrm{y}} = \sqrt{\sigma_{21,\mathrm{y}}^2 + \frac{1}{3}(N_{1,\mathrm{y}}^2 + N_{1,\mathrm{y}} N_{2,,\mathrm{y}} + N_{2,,\mathrm{y}}^2)}. \tag{3-4}$$

Before we proceed to calculate the corresponding yield stresses for each material, we are going to analyze equation A. If we continue with the nondimensionalization using the critical stress $(\sigma_{21,\mathrm{y}})$ as a physical parameter, the following relation is obtained

$$\frac{\sigma_{\mathrm{y}}}{\sigma_{21,\mathrm{y}}} = \sqrt{1 + \frac{1}{3}\left(\frac{N_{1,\mathrm{y}}}{\sigma_{21,\mathrm{y}}}\right)^2 \left(1 + \frac{N_{2,\mathrm{y}}}{N_{1,\mathrm{y}}} + \left(\frac{N_{2,\mathrm{y}}}{N_{1,\mathrm{y}}}\right)^2\right)}. \tag{3-5}$$

which is the nondimensionalized form of the current relation used for simple shear flow adopted in rheology to represent the yield stress, which is the stress level in which bellow no irreversible flow occurs. If we plot the physical quantity $\sigma_{\mathrm{y}}/\sigma_{21,\mathrm{y}}$ as a function of $N_{1,\mathrm{y}}/\sigma_{21,\mathrm{y}}$, for different normal stress ratios $N_{2,\mathrm{y}}/N_{1,\mathrm{y}}$ considering the interval $N_{2,\mathrm{y}}/N_{1,\mathrm{y}} \in$[-1,0], as it can be seen in Figure A, this yield stress relation implicitly has the idea of a negligible effect of $N_{1,\mathrm{y}}$ and $N_{2,\mathrm{y}}$ on the yield stress, in other words, the variation of the ratio $N_{2,\mathrm{y}}/N_{1,\mathrm{y}}$ has almost no effect on the curve presented in Figure 3.18.

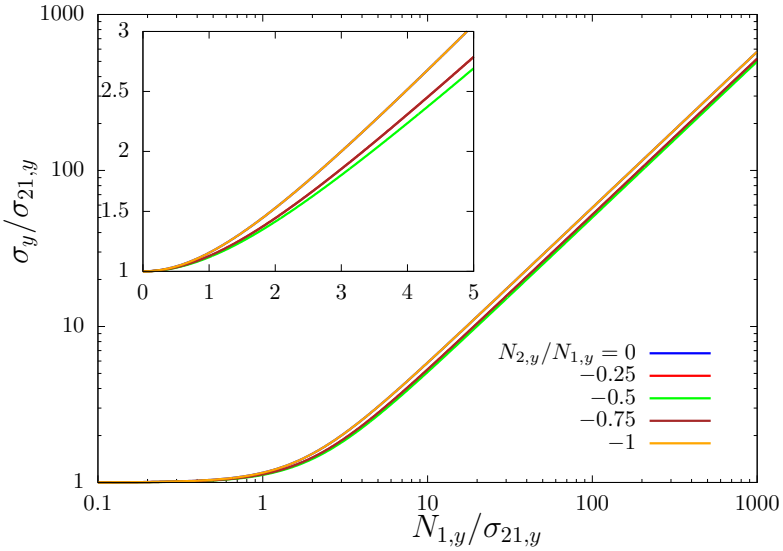


Figure 3.18: The theoretical tendency of the nondimensionalized form of the von Mises yielding criterion for simple shear flow.

However, according to the results obtained for simple shear flow and presented in Table A, it was shown that for the materials studied in the present work we have,

$$\frac{1}{3}(N_{1,\mathrm{y}}^2 + N_{1,\mathrm{y}}N_{2,,\mathrm{y}} + N_{2,,\mathrm{y}}^2) >> \sigma_{21,\mathrm{y}}^2 \tag{3-6}$$

which indicates that the von Mises relation does not see to be accurately representing the yielding phenomenon. Furthermore, it can be speculated that is not just inaccurate for the materials studied but for a vast range of elasto-viscoplastic materials.

Now, assuming that von Mises yielding criterion holds for the materials under study, we are going to calculate the yield stress for each material using the relation 3-4 and compare these results with the yield stresses for the following cases: (i) $N_{1,\mathrm{y}} = N_{2,\mathrm{y}} = 0$, (ii) $N_{1,\mathrm{y}} = 0$, and (iii) $N_{2,\mathrm{y}} = 0$. Additionally, in Tables 3.3 and 3.4, we are going to show the percentual contribution of each simplified case to the yield stress by evaluating each ratio $\sigma_{\mathrm{y}}^{\mathrm{case}}/\sigma_{\mathrm{y}} \times 100$. Among all the materials studied the putty was an exception to the comments that will be made, due to the fact that both $N_{1,\mathrm{y}}$ and $N_{2,\mathrm{y}}$ had a negligible influence on the yield stress estimated in agreement with the von Mises theory. It seems reasonable considering that it is a “solid-like" material and this theory was developed for solids. For the other materials studied the contribution of the critical stress ($\sigma_{21,\mathrm{y}}$) to the yield stress had varied in the interval of (1.84%, 6.13%). The combined influence of $\sigma_{21,\mathrm{y}}$ and $N_{1,\mathrm{y}}$ to the yield stress estimated had fluctuated in a range of (57.18%, 81.49%), what evidences the greater influence of $N_1$. The weight of $N_2$ and $\sigma_{21,\mathrm{y}}$ joined, to the measured yield stress, had ranged in the interval (30.76%, 58.32%), which evidences that

the influence of the $N_{2,y}$ was greater than the one of $\sigma_{21,y}$. Besides, for the majority of the materials[20], the influence of $N_{1,y}$ was greater than $N_{2,y}$, except by the Carbopol® 1% and the solder paste in which the contribution of $N_{2,y}$ was about 1% greater than the N1 contribution to the yield stress evaluated.

Table 3.3: In this table, we show for each material analyzed, using the von Mises yield criterion, the yield stresses estimated based on data previous obtained. Additionally, the simplified cases are shown and analyzed by percentage.

| Materials | $\sigma_y$ (Pa) | $N_{1,y} = N_{2,y} = 0$ (Pa) | $N_{1,y} = 0$ (Pa) |
|---|---|---|---|
| Carbopol® 0.5% | 1538.73 | 61.50 (4.00%) | 674.02 (43.80%) |
| Carbopol® 1.0% | 6611.94 | 121.50 (1.84%) | 3856.40 (58.32%) |
| Comercial hair gel A | 3787.71 | 141.25 (3.73%) | 1877.41 (49.56%) |
| Comercial hair gel B | 3091.58 | 131.25 (4.24%) | 1160.49 (37.54%) |
| Comercial hair gel C | 2220.01 | 136.00 (6.13%) | 682.96 (30.76%) |
| Grease lubrication | 8295.21 | 461.50 (5.56%) | 4257.01 (51.32%) |
| Solder paste | 2139.07 | 105.00 (4.91%) | 1241.29 (58.03%) |
| Putty | 613.15 | 610.50 (99.57%) $= \sigma_{21,y}$ | 610.79 (99.62%) Contributions of $\sigma_{21,y}$ and $N_{2,y}$ |
| **Yield stress** | | | |

Table 3.4: Continuation of the Table 3.3.

| Materials | $N_{2,y} = 0$ (Pa) |
|---|---|
| Carbopol® 0.5% | 1089.52 (70.81%) |
| Carbopol® 1.0% | 3780.87 (57.18%) |
| Comercial hair gel A | 2488.25 (65.69%) |
| Comercial hair gel B | 2350.10 (76.02%) |
| Comercial hair gel C | 1809.16 (81.49%) |
| Grease lubrication | 5331.41 (64.27%) |
| Solder paste | 1234.64 (57.72%) |
| Putty | 612.16 (99.84%) Contributions of $\sigma_{21,y}$ and $N_{1,y}$ |
| **Yield stress** | |

As a partial conclusion, we had experimentally presented results that led us to conclude that for the majority of the materials studied the normal

[20]Excluding the previously commented putty.

stress differences were not negligible and much greater than the critical stresses ($\sigma_{21,y}$). Based on this experimental evidence, it can be speculated that the same is true for a vast range of elasto-viscoplastic materials. In addition, an evidence has been raised that the von Mises criterion seems not to be accurate for the majority of this type of materials representing the yielding phenomenon. In the following chapter, in order to verify the validity of von Mises yielding criterion, we are going to extend the present study verifying the yield stresses for traction and compression flows for each material. Having in mind that the yield stress should be the same regardless the flow type employed in its measurements.

# 4
# PART II - The validity of the von Mises yielding criterion

This chapter is dedicated to the final part of the present research which consists basically in evaluating the validity of the von Mises yielding criterion for elasto-viscoplastic materials. For this purpose, in order to evaluate the yield stress for different flow conditions, constant volume squeeze flow and traction tests were performed. After that, the intensity of the deviatoric stress tensor was calculated for each flow and material estimating the corresponding yield stresses. For all materials investigated, large discrepancies were evidenced by comparing the yield stresses obtained under traction, compression, and the previously obtained simple shear.

Furthermore, for the constant volume squeeze flow measurements, as will be shown in detail as follows, for both no-slip and partial boundary conditions, it was possible to obtain the static equilibrium state for all materials studied. However, due to the complexity of considering the no-slip boundary condition, just for the partial slip boundary condition was possible to estimate the yield stresses. The static equilibrium results and the critical stresses estimated for the no-slip boundary condition can be found in A.



## 4.1
## Squeeze flow

The squeeze flow experiment is defined as a flow in which a sample in a disc-shaped form is compressed between two parallel plates and thus flows radially. The relation between the normal force and the gap that separates the plates was first modeled for a Newtonian fluid in 1874 by (119). As reported by (34), this kind of flow has a vast range of applicability. It can be applied to purely viscous liquids, yield stress materials, purely elastic solids, liquids, viscoelastic solids, and in this section's experiments, for elasto-viscoplastic materials. However, after the development of the capillary and rotational rheometry a limited use of this technique can be seen in the material characterization literature, mainly because of the inherently unsteady, inhomogeneous nature of the flow, with a changing geometry, this issue can be avoided given a low enough velocity and using a quasi-steady state approximation (see chapter 18 of (40)).

Several researchers have done theoretical and numerical studies on this subject, since the pioneers works of (108), (119) and (32), (e.g., (65, 117, 77, 131, 50, 105, 101)), and a reach review can be found in (34). A method to determine the characteristic flow curve from the squeeze film flow experiment for power-law fluid was proposed by (102). The free surface tension was evaluated by (71), a comparison between the orders of magnitude of the internal stresses and the free surface tension was made, concluding that free surface tension can be considered negligible in constant volume squeeze flow tests (CVSF). Although (115) stated based on (116, 79, 65, 80) that the reproducibility of materials such as pastes can be poor in conventional rheometry because the wall slip phenomenon occurs, we are going to show in this work that is it possible to obtain static equilibrium for several materials, including pastes, under partial slip and no-slip boundary conditions and estimate the corresponding yield stresses under compression flow. A Herschel-Bulkley fluid was studied by (106) using stress ramp, two constant stress and CVSF tests for three different concentrations of Carbopol® (1%, 1.5%, and 2%). They performed CVSF tests with no-slip boundary condition using smooth plates and sandpaper covering it. The yield stress estimate was based on a critical interplate separation recorded up to 8 minutes. It is important to mention that the materials analyzed have not reached the static equilibrium as can be seen in its figure 2, instead, a tolerance was adopted. (26) assumed for a pressure gradient generated squeeze flow that the flow resistance is due to shear stress solely for a Bigham fluid with no-slip boundary condition. The normal stress differences of the deviatoric stress tensor were neglected. In contrast, (99) developed a new apparatus in order to perform the no-slip CVSF. Assuming a Herschel- Bulkley model, more specifically, a power law model considering that the stresses in CVSF are larger than the yield stress (their equations 11 and 12). They come up with a linear expression between the cross-section area and time determined by the normal deviatoric stresses, concluding that the Bingham model was a reasonable approximation for CVSF. It is worth to reinforce that they have not achieved static equilibrium condition and, besides the von Mises criterion was assumed to hold, implicitly. A reach and well-discussed review of squeeze flow for nonelastic semi-liquids foods were published by (19). Several results for Newtonian and Non-Newtonian foods from the literature were presented and commented, in which a technique called imperfect squeeze flow was employed to estimate the apparent yield stresses. The latter employs a lower plate in “U" shape which turns it less accurate, the reason is the same as for constant area squeeze flow that is the accumulation of material outside the plate which affects the results. Furthermore, they stated

that "the standard mathematical models, which had been primarily developed for polymers, may not be applicable to at least several important food types. (...)", but they have not explained a possible reason for it.

From an experimental point of view, squeeze flow can be roughly classified into two different types. One of these is known as the sample and plate geometry, in which the sample radius is equal[1] or larger than that of the plates. Even known that the sample position errors are reduced because of the knowledge of the contact area during all the experiment time, as reported by (34) there are some limiting disadvantages, the main ones are: the unknown boundary conditions at the edges of the plates and the difficulty of predicting the variable pressure caused by the accumulation of material outside the plate which affect the results[2]. The other experiment, that was applied in this study, is called the constant volume squeeze flow. In this case, the plates are larger than the sample[3], as well as being closer to industrial compression molding processes. The experiment is done in a way that minimizes the additional pressure build-up around the edges and the stresses are more clearly defined at the edge (see for more details (34)), the only inconvenient procedure is that the contact area needs to be calculated over time.

Our experiments consider the no-slip and partial slip[4], at the plates interfaces, boundary conditions that will be shown separately in Appendix A and in the following subsection. The reason for it is due to the no-slip flow complexity, which would lead us to unphysical assumptions in order to estimate the yield stress. Therefore the yield stress was estimated solely for the partial slip boundary condition. The procedure adopted, in agreement with (93), (71) and (111), consisted of a constant normal force applied to a sample while the gap variation was recorded over time. The latter was due until a static equilibrium state[5] was achieved. Because this experiment is volume preserving[6], we could estimate, by simple geometry, the current contact area and then estimate the critical stress[7] in compression followed by the corresponding yield stress estimation.

A rotational shear stress controlled and Peltier temperature controlled rheometer[8] was employed. For the sake of performing approximately the partial

[1] As in common experiments in rheometry.

[2] At low compression speed (segregation effects.), high viscosity materials and/or at a large room/plate temperature gradient

[3] In a disc-shaped.

[4] Following the nomenclature adopted in (34).

[5] When the sample spreading ceased.

[6] It is worth to reinforce that we adopt a special chamber to avoid evaporation.

[7] It is defined as the ratio between the applied normal force and the current cross-section area of the sample measured at the static equilibrium condition.

[8] Haake Mars III.

slip boundary condition, a coaxial new apparatus was projected which consists of a pair of acrylic smooth plates with 180 mm of diameter, and a mold with 71mm of diameter and 14.7 mm in height (see figures 4.1, 4.2 and 4.3). The experimental preparation procedure adopted pursues the following steps: (a) fit and calibrate the adaptation apparatus, (b) set and calibrate the initial gap and other parameters, (c) fit the mold on the bottom plate of the rheometer, (d) spread the vaseline upon the surface, (e) place the material with a syringe, (f) eliminate excess material, (g) eliminate blisters with the syringe, (h) remove the mold, (i) set the upper plate in contact with the top of the sample, and (j) fit a chamber to avoid evaporation.

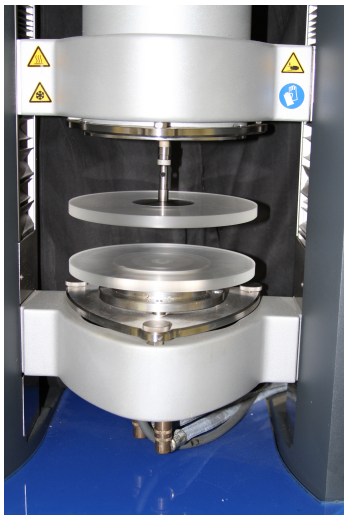

Figure 4.1: Pair of acrylic smooth plates.

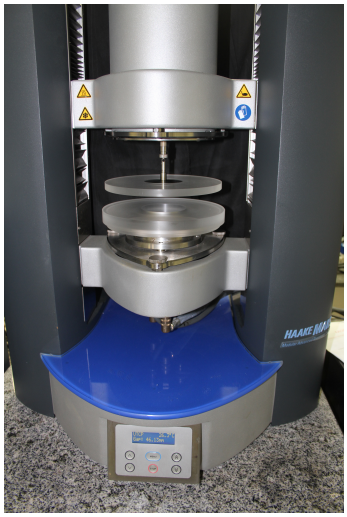

Figure 4.2: Pair of acrylic smooth plates with the mold.

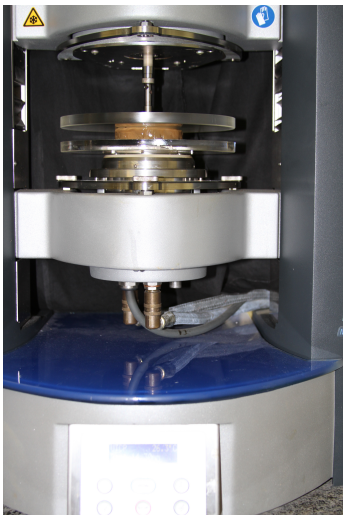

Figure 4.3: Picture of the grease sample.

A constant volume squeeze flow tests were performed, specifically, a constant normal force was employed and the gap separation between plates was recorded over time. According to each material consistency, the following constant values of normal forces were used 1 N (Carbopol® 0.5%, Carbopol® 1.0%, and commercial hair gels A, B, and C), 5 N (grease and solder paste) and 15 N (putty). Although it was not possible to ensure the perfect slip boundary condition, a very close condition was achieved spreading vaseline onto the acrylic smooth plates surface, as can be seen in Figure 4.4(b), in the static equilibrium condition, almost no wall effect can be observed, on the other hand for the no-slip case the plate effect on the sample is noticeable and symmetric (Figure 4.4(a), see Appendix A for further details). The static equilibrium state could be reached for all the materials tested these results are shown in figure 4.5.

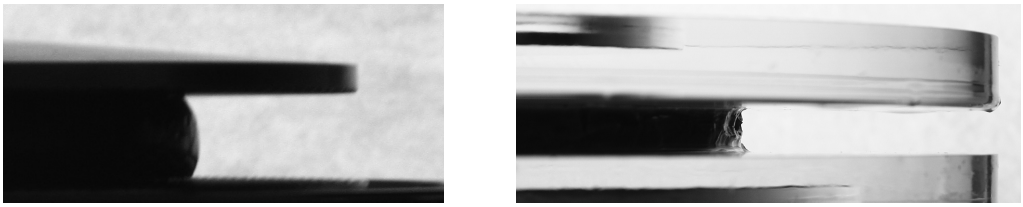

(4.4(a)) No-slip boundary condition. (4.4(b)) Partial slip boundary condition.

Figure 4.4: Constant volume squeeze flow tests.

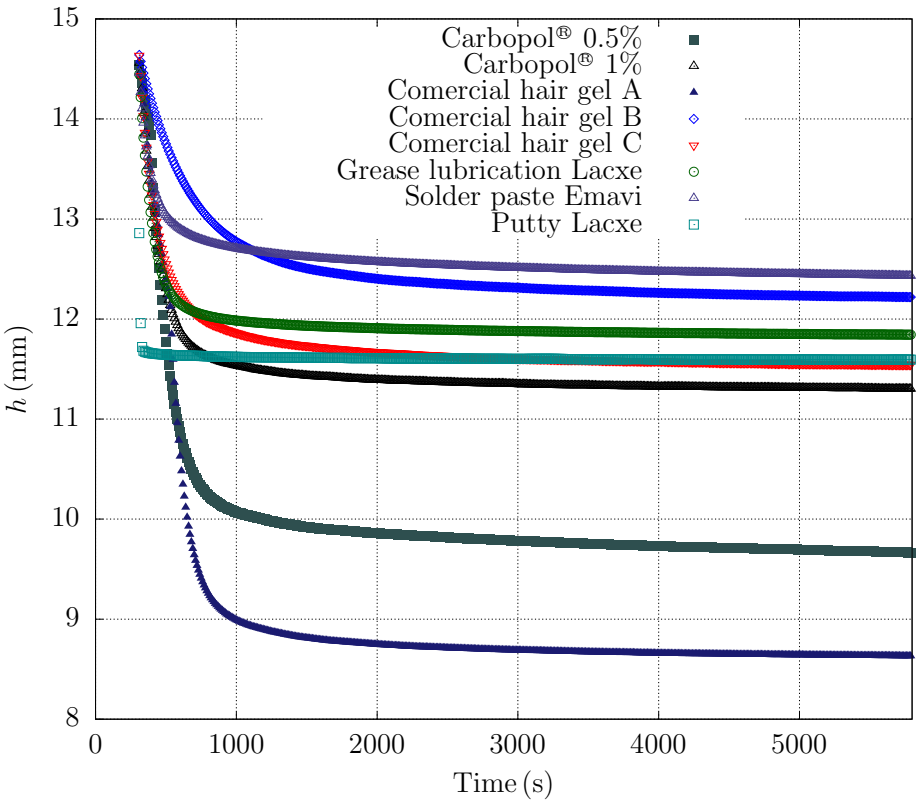


Figure 4.5: Constant volume squeeze flow test, with slip boundary condition.

For all materials, a similar qualitative behavior could be observed. In order to get into details, we are going to classified the materials as: group I (Carbopol® 1%, commercial hair gel C and grease), group II (solder paste, commercial hair gel b), group III (Carbopol® 0.5%, commercial hair gel A) and group IV (putty). The behavior of the gap separation between plates profile over time exhibited the following tendencies: (a) group I materials have displayed a sharp linear decrease with a sudden transition to an asymptotic value, indicating that the materials have reached the static equilibrium, (b) for group II materials, it could be observed a smooth monotonic decreasing profile until stabilized on an asymptotic plateau, (c) the most dramatic drop could be observed in group III materials followed by a smooth transition to the static equilibrium plateau and, (d) for the group IV, the gap profile

displayed a considerable drop followed by an almost direct transition to the static asymptotic plateau. Lastly, as expected, the compressive critical stresses measured under partial slip boundary conditions were considerably lower than the ones measured under no-slip boundary condition, as can be seen at Table 4.1. The reason is due to the fact that the vaseline spread out upon the acrylic plates surfaces created almost no additional friction, in this sense the resistance to the constant compressive load was almost completely due to the materials microstructure.

Table 4.1: In this table, we show for each material analyzed in this work the compressive critical stresses, measured at constant volume squeeze flow test, under no-slip and partial slip boundary conditions.

| Materials | $\sigma_{11,y}$ (No-slip) | $\sigma_{11,y}$ (Partial slip) |
|---|---|---|
| Carbopol® 0.5% | 579.32 | 158.42 |
| Carbopol® 1.0% | 664.21 | 194.16 |
| Comercial hair gel A | 592.06 | 148.11 |
| Comercial hair gel B | 676.94 | 209.79 |
| Comercial hair gel C | 657.84 | 198.11 |
| Grease lubrication | 1402.69 | 1017.18 |
| Solder paste | 1933.20 | 1065.29 |
| Putty | 4439.36 | 2987.11 |
| **Compressive critical stresses - (Pa)** | | |

Turning our attention to the yield stress estimation, we are going to proceed similarly as in section 3.4. Considering the situation in which the sample had reached the static equilibrium state, the force balance at the upper plate (see figure 4.6) is represented by

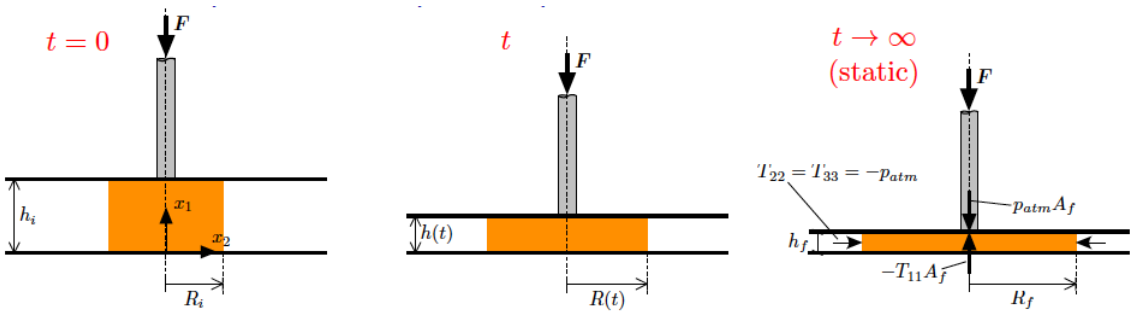


Figure 4.6: Squeeze flow.

$$-T_{11}A_f - p_{\text{atm}}A_f - F = 0 \Rightarrow (T_{11} + p_{\text{atm}})A_f = -F \Rightarrow T_{11} - T_{22} = -\frac{F}{A_f} \quad (4\text{-}1)$$

where $A_f$ is the current cross-section area of the upper plate, F is the normal force applied and $p_{\text{atm}}$ the atmospheric pressure. As a result of the axial symmetry and the perfect wall slip boundary condition the stress state is characterized as follows

$$\boldsymbol{T} = \begin{bmatrix} T_{11} & 0 & 0 \\ 0 & T_{22} & 0 \\ 0 & 0 & T_{33} \end{bmatrix}.$$

where $T_{22} = T_{33}$ and $T_{12} = T_{21} = T_{13} = T_{31} = T_{23} = T_{32} = 0$. Using the deviatoric stress definition,

$$\boldsymbol{\sigma} = \boldsymbol{T} - \left(\frac{1}{3}\text{tr}\boldsymbol{T}\right)\boldsymbol{I} = \boldsymbol{T} - \frac{1}{3}(T_{11} + 2T_{22})\boldsymbol{I} \quad (4\text{-}2)$$

$$\text{Thus, } \begin{cases} \sigma_{11} = T_{11} - \frac{1}{3}(T_{11} + 2T_{22}) = \frac{2}{3}(T_{11} - T_{22}) \\ \sigma_{22} = T_{22} - \frac{1}{3}(T_{11} + 2T_{22}) = -\frac{1}{3}(T_{11} - T_{22}) \\ \sigma_{33} = \sigma_{22} \\ \sigma_{ij} = T_{ij} = 0 \text{ when } i \neq j \end{cases}$$

Therefore, the deviatoric stress is expressed as

$$\boldsymbol{\sigma} = \begin{bmatrix} \frac{2}{3}(T_{11} - T_{22}) & 0 & 0 \\ 0 & -\frac{1}{3}(T_{11} - T_{22}) & 0 \\ 0 & 0 & -\frac{1}{3}(T_{11} - T_{22}) \end{bmatrix}.$$

Consequently,

$$\boldsymbol{\sigma^2} = \begin{bmatrix} \frac{4}{9}(T_{11} - T_{22})^2 & 0 & 0 \\ 0 & \frac{1}{9}(T_{11} - T_{22})^2 & 0 \\ 0 & 0 & \frac{1}{9}(T_{11} - T_{22})^2 \end{bmatrix}.$$

Therefore, using equation 2-11, the von Mises stress can be calculated as follows

$$\sigma_v = \sqrt{\frac{1}{2}\text{tr}(\boldsymbol{\sigma}^2)} = \frac{|T_{11} - T_{22}|}{\sqrt{3}} \quad (4\text{-}3)$$

Lastly, applying the relation 4-1, previously obtained from the force balance, the yield stress of this flow can be obtained througth the following relation

$$\sigma_{\text{y}} = \frac{F/A_f}{\sqrt{3}}. \quad (4\text{-}4)$$

The corresponding yield stresses estimated for each material are presented in table 4.2.

Table 4.2: In this table we show for each material analyzed in this work the yield strengths and critical lengths under partial slip boundary condition.

| Materials | $\sigma_y$ (Pa) | Critical length (mm) |
|---|---|---|
| Carbopol® 0.5% | 91.46 | 9.22 |
| Carbopol® 1.0% | 112.10 | 11.3 |
| Comercial hair gel A | 85.51 | 8.62 |
| Comercial hair gel B | 121.12 | 12.21 |
| Comercial hair gel C | 114.38 | 11.53 |
| Grease lubrication | 587.27 | 11.84 |
| Solder paste | 615.04 | 12.4 |
| Putty | 1724.61 | 11.59 |
| **Partial slip constant volume squeeze flow** | | |
| Initial gap ($mm$) | 14.7 | |
| Initial diameter ($mm$) | 71 | |
| Cross hatched plates diameter($mm$) | 180 | |

## 4.2 Traction flow

The idea behind this experiment is to approximately perform a traction test in order to estimate the yield stress for a flow induced by a tension load. For this purpose, an experimental apparatus was developed with the following elements: test section, pump, water reservoir, camera and balance (see figures 4.7 and 4.8). A preliminary test was performed with a syringe-like reservoir in which the fluid was submitted to a load caused by the piston[9] weight. The lowest possible velocity value that could be measured without practical problems[10] were used to calibrate the water pump and scale out the new reservoir dimensions. The experimental preparation procedure adopted pursues the following steps: (a) adjust the camera, (b) place the material with a syringe filling the space below the piston, (c) eliminate blisters with a syringe, (d) assemble the piston and the top of the reservoir, (e) set and calibrate the water pump and the frequency inverter, (f) water is pumped into the space above the piston, to force it down, (g) the piston speed is controlled by the pump rotation, (h) the sample exits vertically from an orifice at the bottom cap, (i) the filament breaks due to gravity, (j) the filament motion and breakage is recorded, and (l) the detached filament length is obtained via image analysis.

[9]This piston was machined with one of the ends in a conical shape with a characteristic angle of 56 °.

[10]Problems of geometry interference showed up under small velocities.

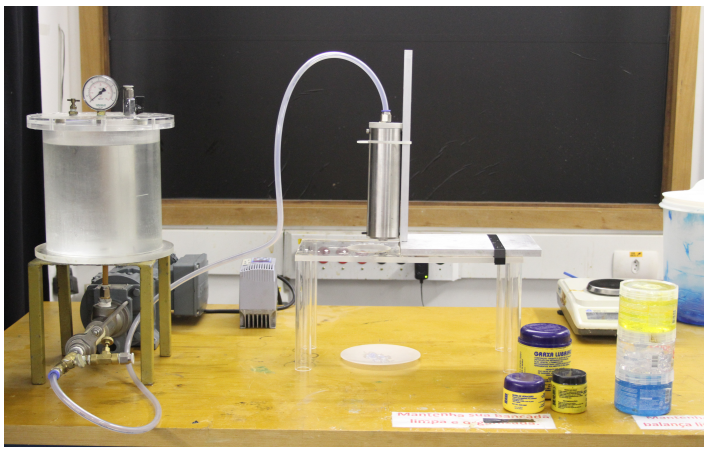

Figure 4.7: Traction experimental apparatus.

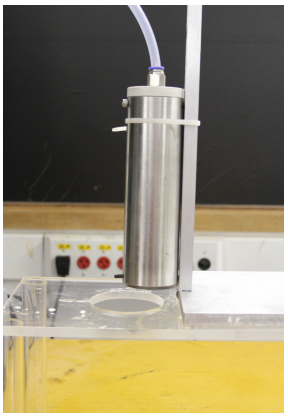

Figure 4.8: Syringe-like reservoir.

The subsequent filament thinning process was captured by a high-speed camera EOS 7D (BRAND Canon) with a sampling speed of 30 frames per second. The resolution of each frame was 1920 x 1080 pixels with Canon EF 100mm lens F2.8L Macro IS USM. To improve contrast, the fluid filament was illuminated from the back and the front with a led light type illumination. For each experiment, several videos were regularly recorded until the filament breakup. Image analysis provided the velocity, the criticals diameters, and length[11] for each of the sequences of tests varying the velocity. Then, fitting the experimental data with polynomial regression we could extrapolate to the zero velocity, eliminating any material memory efects, to estimate the limit of the critical length values for eache material (see figures 4.9, 4.10, 4.11, 4.12, 4.13, 4.14, 4.15 and 4.16.). In view of making it clear, it is important to mention that each point at each plot represents an extremely time-consuming experiment.

[11]It is defined as the length in which the material starts to deform. We made the assumption that the material starts to deform when the difference in between the initial material characteristic diameter and the lowest current diameter over all the sample was equal or bigger than $10^{-3}$ mm.

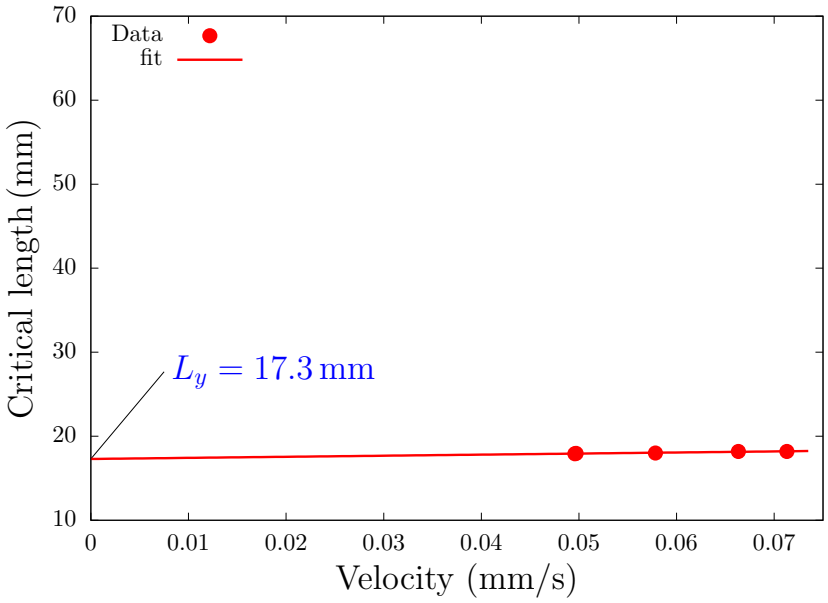


Figure 4.9: Results of several traction experiments with different velocities and recording the corresponding critical lengths for Carbopol® 0.5%.

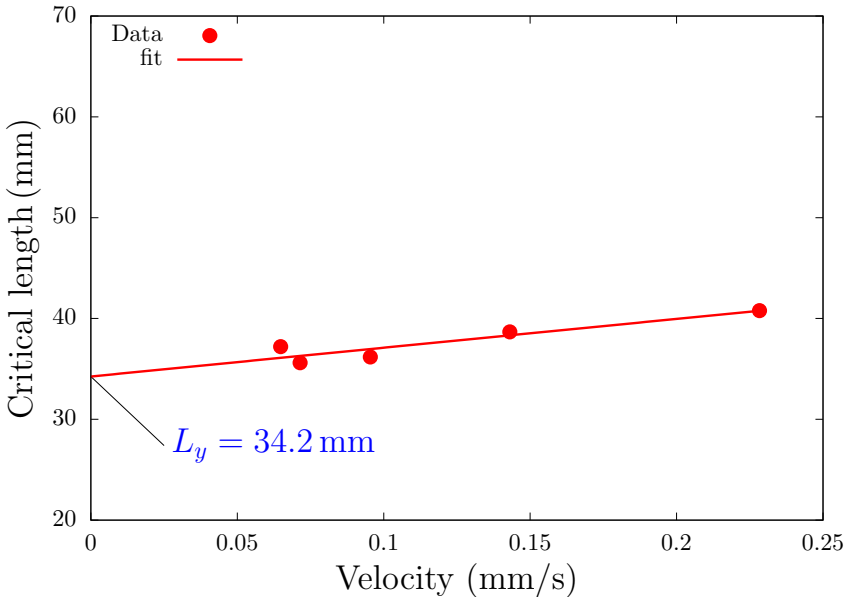


Figure 4.10: Results of several traction experiments with different velocities and recording the corresponding critical lengths for Carbopol® 1%.

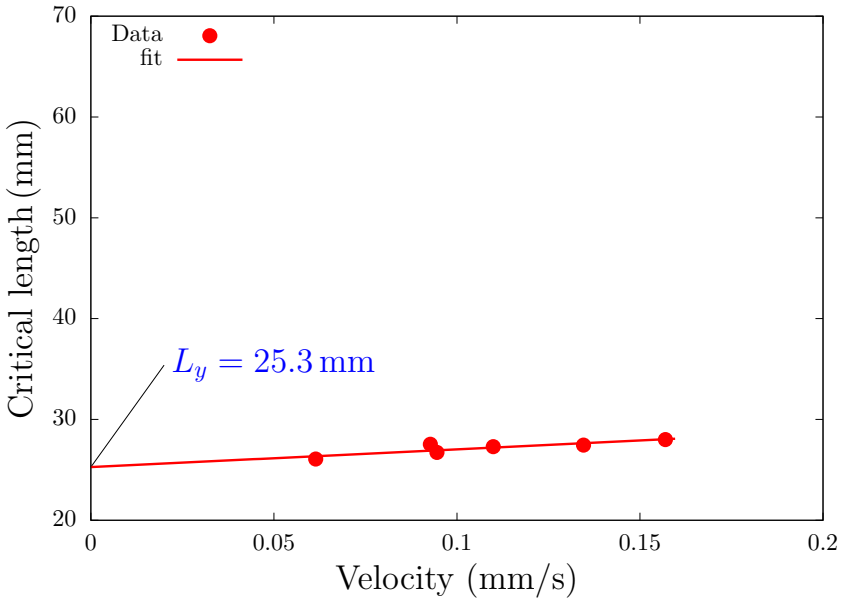


Figure 4.11: Results of several traction experiments with different velocities and recording the corresponding critical lengths for commercial hair gel A.

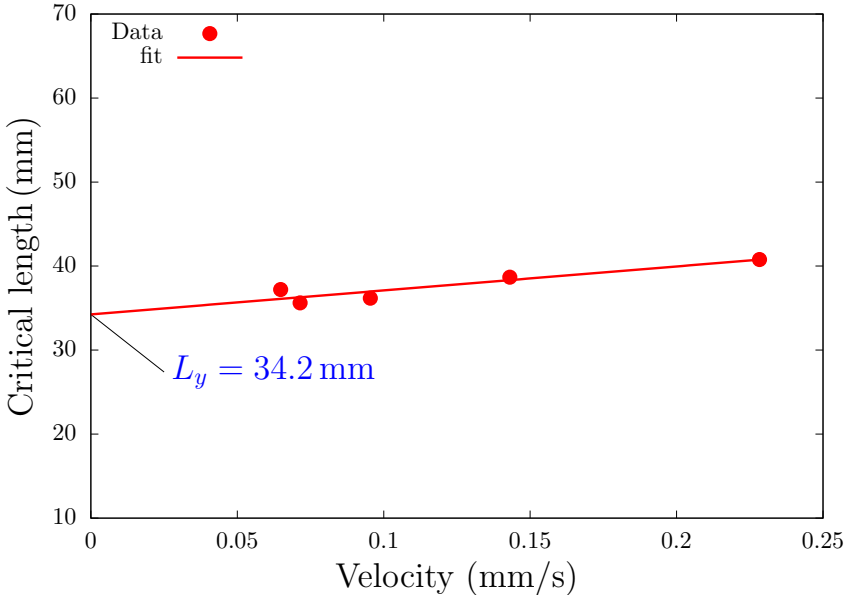


Figure 4.12: Results of several traction experiments with different velocities and recording the corresponding critical lengths for commercial hair gel B.

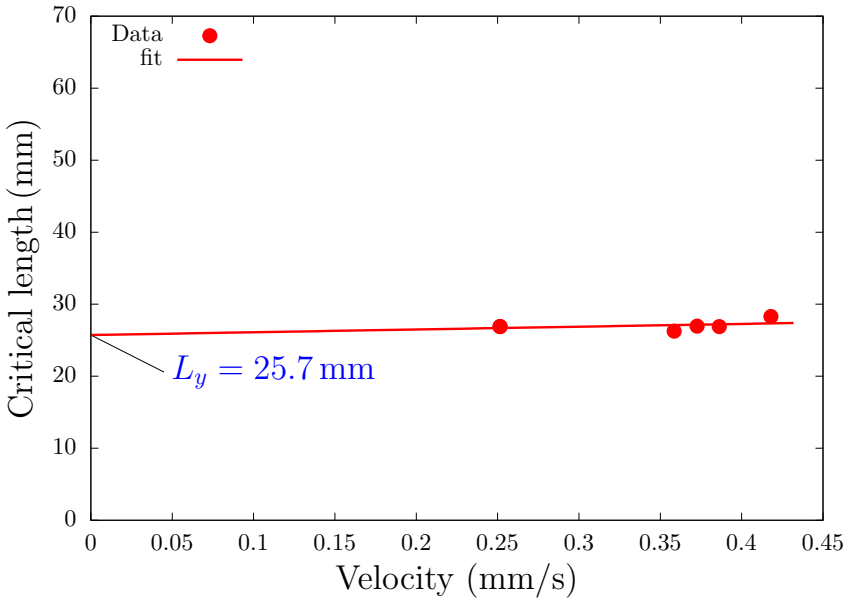


Figure 4.13: Results of several traction experiments with different velocities and recording the corresponding critical lengths for commercial hair gel C.

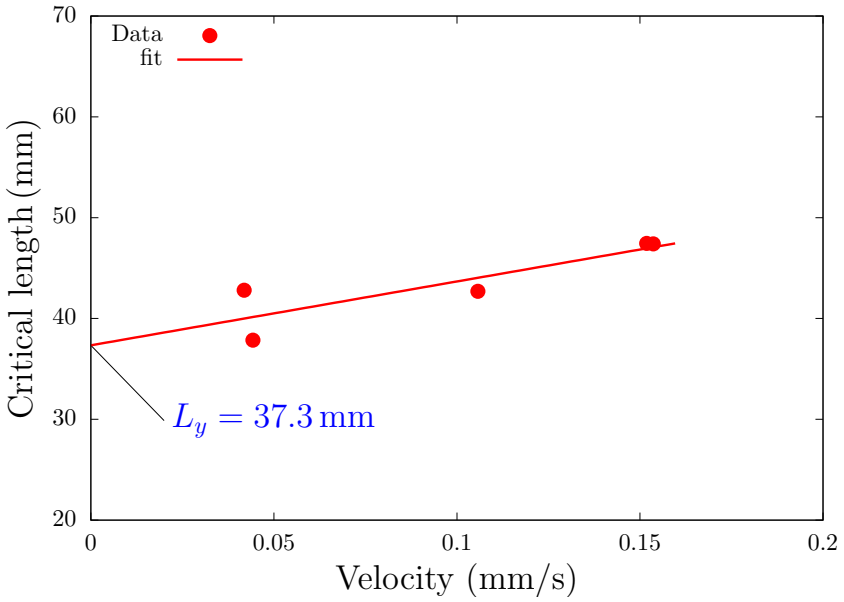


Figure 4.14: Results of several traction experiments with different velocities and recording the corresponding critical lengths for grease.

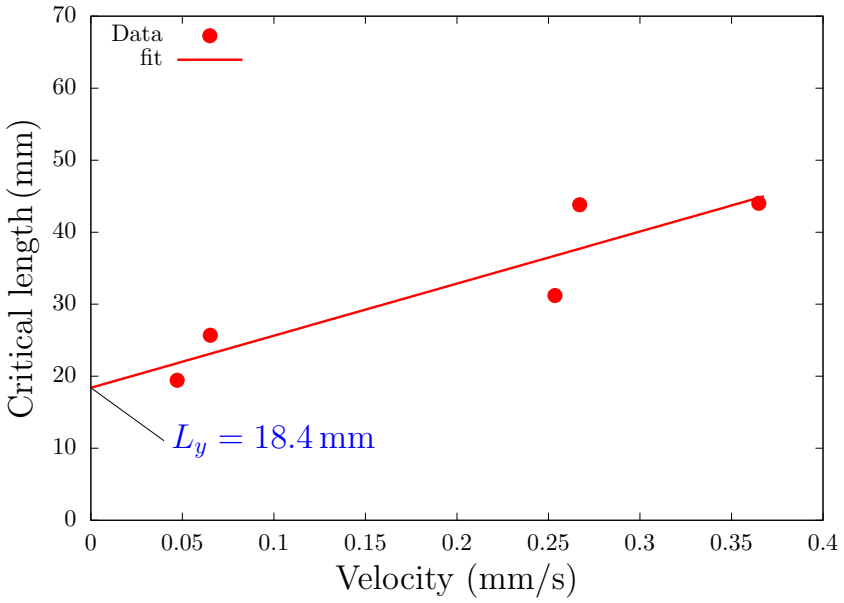


Figure 4.15: Results of several traction experiments with different velocities and recording the corresponding critical lengths for solder paste.

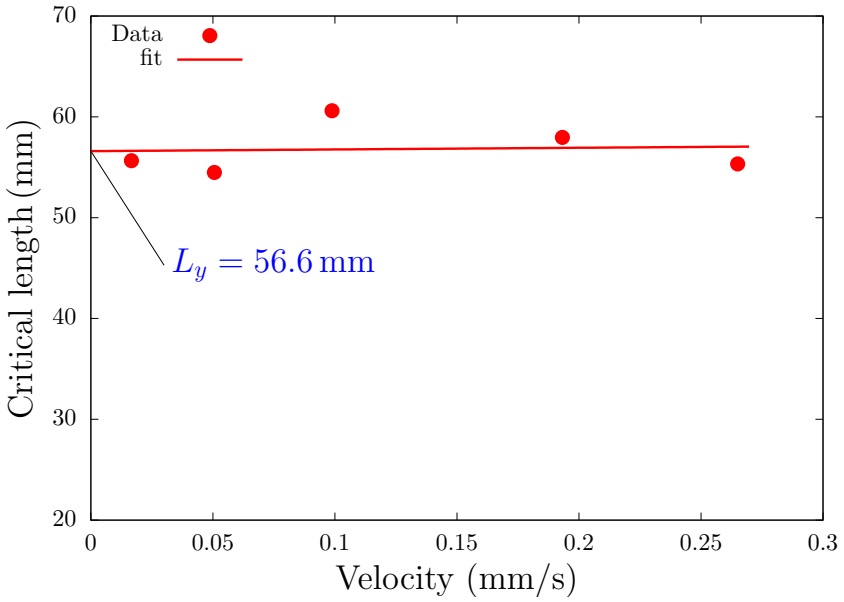


Figure 4.16: Results of several traction experiments with different velocities and recording the corresponding critical lengths for putty.

As expected most of the materials studied have shown a linear behavior, expected by the putty in which the velocity gradient seemed had no effect on the critical length. In possession of the critical length values, we are going to perform a straightforward force balance in order to evaluate the first normal stress difference. After that, using the definition the deviatoric stress tensor we are going to estimate for each material the corresponding yield stresses. Let us consider a control volume and forces acting on it as shown in Figure 4.17,

assuming an equilibrium state in the $x_1-$direction we have

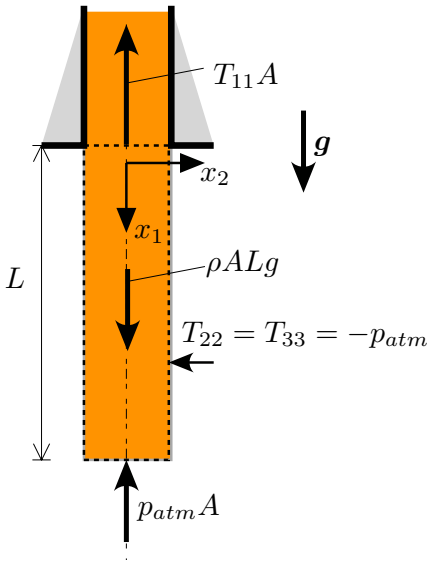


Figure 4.17: Control volume.

$$\rho gLA - p_{\text{atm}}A = T_{11}A \rightarrow \rho gL + T_{22} = T_{11} \rightarrow T_{11} - T_{22} = \rho gL \qquad (4\text{-}5)$$

where g is the component of the acceleration of gravity in the $x_1-$direction, L is the characteristic length, A is the cross-section area and $\rho$ is the material density. Related to the $x_1-$direction the deviator normal stress differences become

$$\begin{cases} \sigma_{11} - \sigma_{22} = T_{11} - T_{22} = \rho gL \\ \sigma_{22} - \sigma_{33} = T_{22} - T_{33} = 0 \end{cases}$$

By the deviator stress tensor definition, its trace[12] is zero which leads us to conclude that, $\sigma_{11} = \frac{2}{3}\rho gL$ and $\sigma_{22} = \sigma_{33} = -\frac{1}{3}\rho gL$. Tensorially,

$$\boldsymbol{\sigma} = \begin{bmatrix} \frac{2}{3} & 0 & 0 \\ 0 & -\frac{1}{3} & 0 \\ 0 & 0 & -\frac{1}{3} \end{bmatrix} \rho gL$$

Consequently,

$$\boldsymbol{\sigma^2} = \begin{bmatrix} \frac{4}{9} & 0 & 0 \\ 0 & \frac{1}{9} & 0 \\ 0 & 0 & \frac{1}{9} \end{bmatrix} \rho^2 g^2 L^2 \rightarrow$$

[12] $\text{tr}(\boldsymbol{\sigma}) = \sigma_{11} + \sigma_{22} + \sigma_{33} = 0$.

Therefore, using equation 2-11, the von Mises stress can be calculated as follows

$$\sigma_v = \sqrt{\frac{1}{2}\mathrm{tr}(\boldsymbol{\sigma}^2)} = \frac{\rho g L}{\sqrt{3}} \tag{4-6}$$

So, for this flow the yield stress is given by

$$\sigma_v = \frac{\rho g L_y}{\sqrt{3}} \tag{4-7}$$

where $L_y$ is the maximum length that the extrudate attains before breaking, in the limiting situation of zero flow. The tensile yield stresses and the corresponding critical lengths are shown in table 4.3.

Table 4.3: In this table we show for each material analyzed in this work the tensile yield stresses.

| Materials | $\sigma_y$ (Pa) | Critical length (mm) |
|---|---|---|
| Carbopol® 0.5% | 97.69 | 17.30 |
| Carbopol® 1.0% | 194.18 | 34.24 |
| Comercial hair gel A | 143.04 | 25.27 |
| Comercial hair gel B | 193.17 | 34.24 |
| Comercial hair gel C | 146.25 | 25.70 |
| Grease lubrication | 217.15 | 38.43 |
| Solder paste | 87.86 | 18.40 |
| Putty | 447.78 | 56.60 |
| **Tensile test** | | |

It is worth to mention that, the procedure adopted to determine the respective densities[13] for each material follows the norm “Laboratory glassware - One-mark volumetric flasks ISO 3696". The latter consists of the following procedure: (i) weigh the pycnometer and note the value of the corresponding mass, (ii) fill the pycnometer with deionized water as previously described and weigh it, (iii) with this data knowing the volume of the pycnometer the density is calculated. It is important to note that the pycnometer is filled to the top carefully in order to avoid air bubble formation. Insert the lid or thermometer and carefully remove the excess water overflowing and wet the outside of the pycnometer with absorbent paper. All excess water must be removed, otherwise, the value found at the weighing will be different from the actual one.

[13]Except for the grease, solder paste, and putty in which the measurements were provided by the manufacturers.

## 4.3 Discussion

This section will be dedicated to discussing the discrepancies encountered in the yield stress values measured in simple shear flow, constant volume squeeze flow, and traction flow. The latter was estimated assuming that the von Mises theory was capable of accurately represents the yielding phenomenon of elasto-viscoplastic materials. For this purpose, three yield stress comparisons among the types of flow analyzed in this work will be performed. The first comparability will be accomplished between the extensional yield stresses obtained, the yield stresses of the constant volume squeeze flow and the traction flow, as well as the ratio between them for each material, these results are shown at Table 4.4.

Table 4.4: In this table we show for each material analyzed the measured extensional yield stresses and its ratio.

| Materials | $\sigma_y$ (traction) (Pa) | $\sigma_y$ (compression) (Pa) | Traction/Comp. |
|---|---|---|---|
| Carbopol® 0.5% | 97.69 | 91.46 | 1.07 |
| Carbopol® 1.0% | 194.18 | 112.10 | 1.73 |
| Comercial hair gel A | 143.04 | 85.51 | 1.67 |
| Comercial hair gel B | 193.17 | 121.12 | 1.59 |
| Comercial hair gel C | 146.25 | 114.38 | 1.28 |
| Grease lubrication | 217.15 | 587.27 | 0.37 |
| Solder paste | 87.86 | 615.04 | 0.14 |
| Putty | 447.78 | 1724.61 | 0.26 |
| **Yield stress ratio** | | | |



It was observed small discrepancies among the obtained yield stresses for all the materials studied, indicating that their yield stresses under traction flow and squeeze flow are different. The latter contradicts the von Mises theory in which the yield stress should be the same regardless the type of flow measured, the latter is a consequence of assuming the intensity of the deviatoric stress tensor (equation 2-11) as the scalar intrinsic material property which indicates the level of energy in which the material starts to yield. Interestingly, the results suggest that for polymeric gels the yield stress in traction is larger than in compression, and for concentrated suspensions and emulsion the opposite is true.

The second comparison will be performed between the yield stresses obtained for simple shear flow, considering the first and second normal stress

differences contributions and, the yield stresses obtained for traction flow. The results are presented in Table 4.5.

Table 4.5: In this table, we show for each material analyzed the measured yield stresses of traction flow and simple shear flow and, its ratio.

| Materials | $\sigma_y$ (simple shear) (Pa) | $\sigma_y$ (traction) (Pa) | Simple shear/Traction |
|---|---|---|---|
| Carbopol® 0.5% | 1538.73 | 97.69 | 15.75 |
| Carbopol® 1.0% | 6611.94 | 194.18 | 34.06 |
| Comercial hair gel A | 3787.71 | 143.04 | 26.48 |
| Comercial hair gel B | 3091.58 | 193.17 | 16.00 |
| Comercial hair gel C | 2220.01 | 39.71 | 15.18 |
| Grease lubrication | 8295.21 | 217.15 | 38.20 |
| Solder paste | 2139.07 | 87.86 | 24.35 |
| Putty | 613.15 | 447.78 | 1.37 |
| **Yield stress ratio** | | | |

Several aspects of these result should be commented. Firstly, extremely high values of yield stresses were obtained in simple shear flow, which leads us to unphysical predictions, e.g., yield stresses for polymer gels varying from 1538 to 6611 Pa. Besides, the von Mises theory approach predicted higher values of yield stress for polymer gels than for the putty with a very “solid" consistency which seems unreasonable. Furthermore, comparing these results with the ones for traction flow. The von Mises criterion values of simple shear flow from the yield stress were from 15 to 38 times higher than the ones from traction flow, which should be the same regardless the flow type. Related to the predictions the lowest error encountered, i.e., the material which showed the yield stress ratio closer to one was the commercial putty. The latter seems intuitive based on the fact that the von Mises theory was developed mainly for solids and the putty among all the materials in the one which displays a “solid like" consistency. Similar conclusions can be obtained from Table 4.6.

Table 4.6: In this table, we show for each material analyzed the measured yield stresses of squeeze flow and simple shear flow and, its ratio.

| Materials | $\sigma_y$ (simple shear) (Pa) | $\sigma_y$ (compression) (Pa) | Simple shear/Comp. |
|---|---|---|---|
| Carbopol® 0.5% | 1538.73 | 91.46 | 16.82 |
| Carbopol® 1.0% | 6611.94 | 112.10 | 58.98 |
| Comercial hair gel A | 3787.71 | 85.51 | 44.29 |
| Comercial hair gel B | 3091.58 | 121.12 | 25.52 |
| Comercial hair gel C | 2220.01 | 114.38 | 19.41 |
| Grease lubrication | 8295.21 | 587.27 | 14.13 |
| Solder paste | 2139.07 | 615.04 | 3.48 |
| Putty | 613.15 | 1724.61 | 0.36 |
| **Yield stress ratio** | | | |

Similar conclusions were obtained comparing the yield stresses estimated for simple shear flow and constant volume squeeze flow. Lastly, it seems reasonable for the materials studied to conclude that, the von Mises theory most commonly adopted in Rheology in conjunction with Non-newtonian constitutive relations, is not accurately representing the yielding phenomenon. For extensional flows, the yield stresses ratios were closer to one, indicating that the error was lower. However, the should be the same by definition. By the time we adopted this theory to estimate the yield stress for simple shear flow, extremely higher values were obtained when normal stresses were considered, which permits us to speculate that a more appropriate yielding criterion for elasto-viscoplastic liquids is needed in Rheology.

# 5
# Final remarks and future work

In the first part of the present research, our observations have shown that it is not reasonable, for the materials studied, neglect the normal stress differences contribution to the yield stress estimation under simple shear flow. The latter is a common procedure adopted in Rheology for material characterization. The main aspects of these observations are summarized below:

1. Although the von Mises theory has implicitly modeled the yield stress with a small dependence on the normal stress differences, as shown and commented in section 3.3 (see Figure 3.18). We could observe the opposite behavior which evidenced

$$\frac{1}{3}(N_{1,\mathrm{y}}^2 + N_{1,\mathrm{y}}N_{2,,\mathrm{y}} + N_{2,,\mathrm{y}}^2) >> \sigma_{21,\mathrm{y}}^2.$$

2. We had perceived that the contributions to the yield stress estimation of $N_{1,\mathrm{y}}$ were considerably higher than the one of $\sigma_{21,\mathrm{y}}$.

3. The contribution of $N_{2,\mathrm{y}}$ was also considerably higher than the one of $\sigma_{21,\mathrm{y}}$.

4. For the majority of the materials tested the contributions to the yield stress of $N_{1,\mathrm{y}}$ were higher than the from $N_{2,\mathrm{y}}$.

In the last part of this research, we have demonstrated by experimental evidence, for the materials analyzed, that the von Mises criterion was not accurately representing the yielding phenomenon of elasto-viscoplastic fluids. To reach this conclusion, we had performed measurements of constant volume squeeze flow and traction flow and compared the yield stresses estimated between them and with the results previously obtained for simple shear flow. Large discrepancies were evidenced, and the main conclusions are listed as follows:

1. Comparing the yield stresses obtained for traction flow and constant volume squeeze flow. It was encountered small discrepancies between

them. Interestingly, the results had suggested that for polymeric gels the yield strength in traction is larger than in compression, and for concentrated suspensions and emulsion the opposite is true.

2. Extremely high discrepancies were evidenced comparing the yield stress estimated for simple shear flow with the ones for extensional flows. The results had varied from 3.5 to 58 times higher than the ones for extensional flows.

3. As expected, due to its “solid like" consistency, the commercial putty was the material in which the von Mises theory could be a reasonable approach for yielding. The latter is based on the fact that it had shown a negligible effect of the values of N1 and N2 on the yield stress estimated for simple shear flow. Furthermore, the yield stresses ratios for different flow conditions were close to one.

Finally, our evidence had highlighted the significance of considering the normal stress differences on yield stress estimation for simple shear flow. Furthermore, for the materials tested, the von Mises yield criterion which is widely accepted as appropriate for material characterization in rheology, was considered inaccurate predicting yielding leading to unphysical predictions with different values for different flow conditions. Based on the presented evidence, we could speculate that for the majority of the elasto-viscoplastic fluids it is needed a more appropriate yielding criterion. As a future work, a further experimental investigation should be done, and first theoretical steps in the direction to the development of a new yielding criterion will be taken maybe thinking of the yield stress as a tensorial quantity that describes qualitatively the microstructural characteristics of the material subjected to different kinds of load instead of a scalar intrinsic property (30).

# Bibliography


[1] ABDEL-KHALIK, S. I.; HASSAGER, O. ; BIRD, R. B.. **Prediction of melt elasticity from viscosity data**. Polymer Engineering & Science, 14:859–867, 1974.

[2] ADAMS, N.; LODGE, A. S.. **Rheological properties of concentrated polymer solutions ii. a cone-and-plate and parallel-plate pressure distribution apparatus for determining normal stress differences in steady shear flow**. Philosophical Transactions of the Royal Society of London, 256(1068):149–184, 19 March 1964.

[3] AIT-KADI, A.; CHOPLIN, L. ; CARREAU, P. J.. **On correlations of primary normal stresses in polymer solutions**. Polymer Engineering & Science, 29:1265–1272, September 1989.

[4] ALAM, M.; LUDING, S.. **First normal stress difference and crystallization in a dense sheared granular fluid**. Physics of Fluids, 15(8):2298–2312, 2003.

[5] ALVAREZ, G. A.; CANTOW, H. J.. **Oscillatory normal stresses in melts and concentrated solutions of cis-l,4-polybutadiene**. Polymer Bulletin, 7:51–58, 1982.

[6] ASTARITA, G.. **The engineering reality of the yield stress**. J. Rheol., 34(2):275–277, 1990.

[7] ATTANE, P.; ROY, P. L.; PIERRARD, J. M. ; TURREL, G.. **Memory-function determination of viscoelastic fluids based on relaxation tests (normal and shear stresses)**. Journal of Non-Newtonian Fluid Mechanics, 3:1–12, September 1977.

[8] BAGLEY, E. B.; DUFFEY, H. J.. **Recoverable shear strain and the barus effect in polymer extrusion**. Transactions of The Society of Rheology, 14(545), 1970.

[9] BAIRD, D. G.; READ, M. D. ; PIKE, R. D.. **Comparison of the hole pressure and exit pressure methods for measuring polymer melt normal stresses**. Polymer Engineering & Science, 26:225–232, Feb 1986.

[10] BARNES, H. A.. **Thixotropy - a review**. J. Non-Newtonian Fluid Mech., 70:1–33, 1997.

[11] BARNES, H. A.. **The yield stress-a review**. J. Non-Newtonian Fluid Mech., 81:133–178, 1999.

[12] BARNES, H. A.; WALTERS, K.. **The yield stress mith?** Rheol. Acta, 24:323–326, 1985.

[13] BERTOLA, V.; BERTRAND, F.; TABUTEAU, H.; BONN, D. ; COUSSOT, P.. **Wall slip and yielding in pasty materials**. Journal of Rheology, 47(5):1211–1226, 2003.

[14] BIRD, R. B.; ARMSTRONG, R. C. ; HASSAGER, O.. **Dynamics of polymeric liquids**, volumen 1. Wiley, 1987.

[15] BIRD, R. B.; DOTSON, P. J. ; JOHNSON, N. L.. **Polymer solution rheology based on a finitely extensible bead—spring chain model**. Journal of Non-Newtonian Fluid Mechanics, 7:213–235, 1980.

[16] BRIDGMAN, P. W.. **The compressibility of thirty metals as a function of pressure and temperature**. Proceedings of the American Academy of Arts and Sciences, 58:165–242, 1923.

[17] BRIDGMAN, P. W.. **Studies in large plastic flow and fracture with special emphasis on the effects of hydrostatic pressure**. McGraw-Hill, 1952.

[18] BRIZITSKY, V. I.; VINOGRADOV, G. V.; ISAEV, A. I. ; PODOLSKY, Y. Y.. **Polarization-optical investigation of normal and shear stresses in flow of polymers**. Journal of Applied Polymer Science, 20:25–40, 1976.

[19] CAMPANELLA, O. H.; PELEG, M.. **Squeezing flow viscometry for nonelastic semiliquid foods — theory and applications**. Critical Reviews in Food Science and Nutrition, 42(3):241–264, may 2002.

[20] CARREAU, P. J.. Tese de Doutorado, University of Wisconsin, 1968. Eq. 12-4, p.78.

[21] CARTER, L. F.. **A study of the rheology of the suspensions of rod-shaped particles in a Navier-Stokes liquid**. Tese de Doutorado, University of Michigan, Ann Arbor, MI, 1967.

[22] CATO, A. D.; EDIE, D. D. ; HARRISON, G. M.. **Steady state and transient rheological behavior of mesophase pitch, part i: Experiment**. Journal of Rheology, 49(1):161–174, 2005.

[23] CHAN, Y.; WHITE, J. L. ; OYANAGI, Y.. **A fundamental study of the rheological properties of glass-fiber-reinforced polyethylene and polystyrene melts**. Journal of Rheology, 22:507–524, 1978.

[24] COLEMAN, B. D.; MARKOVITZ, H.. **Asymptotic relations between shear stresses and normal stresses in general incompressible fluids**. Journal of Polymer Science, 12:2195–2207, November 1974.

[25] COUSSOT, P.. **Rheometry of Pastes, suspensions, and granular materials**. Willey-Interscience, 2005.

[26] COVEY, G.; STANMORE, B.. **Use of the parallel-plate plastometer for the characterisation of viscous fluids with a yield stress**. Journal of Non-Newtonian Fluid Mechanics, 8(3-4):249–260, jan 1981.

[27] DE CAGNY, H. C. G.; VOS, B. E.; VAHABI, M.; KURNIAWAN, N. A.; DOI, M.; KOENDERINK, G. H.; MACKINTOSH, F. C. ; BONN, D.. **Porosity governs normal stresses in polymer gels**. Phys. Rev. Lett., 117:217802, Nov 2016.

[28] DE SOUZA MENDES, P. R.; THOMPSON, R.. **A critical overview of elasto-viscoplastic thixotropic modeling**. J. Non-Newtonian Fluid Mech., 187-188:8–15, 2012.

[29] DE SOUZA MENDES, P. R.; THOMPSON, R.. **A unified approach to model elasto-viscoplastic thixotropic yield-stress materials and apparent yield-stress fluids**. Rheol. Acta, 52:673–694, 2013.

[30] DE SOUZA MENDES, P. R.; THOMPSON, R. ; RAJAGOPAL, K. R.. **A thermodynamic framework to model thixotropic materials**. Journal of Non-Linear Mechanics, 55:48–54, 2013.

[31] DHONT, J. K. G.. **An Introduction to Dynamics of Colloids**. Elsevier Science, 1996.

[32] DIENES, G. J.; KLEMM, H. F.. **Theory and application of the parallel plate plastometer**. Journal of Applied Physics, 17(6):458–471, jun 1946.

[33] D.V. BOGER, K. W.. **Rheological Phenomena in Focus**. Elsevier Science, 2012.

[34] ENGMANN, J.; SERVAIS, C. ; BURBIDGE, A. S.. **Squeeze flow theory and applications to rheometry: A review**. J. Non-Newtonian Fluid Mech., 132:1–27, 2005.

[35] FAITELŚON, L. A.; ALEKSEENKO, A. I.. **Effect of filling on the first difference of the normal stresses in a melt of low-density polyethylene with steady-state shear flow**. Polymer Mechanics, 6:490–491, May 1970.

[36] FANG, Y.; TAKEMASA, M.; KATSUTA, K. ; NISHINARI, K.. **Rheology of schizophyllan solutions in isotropic and anisotropic phase regions**. Journal of Rheology, 48(5):1147–1166, 2004.

[37] FREUNDLICH, H.. Número 46-289. 1929.

[38] FREUNDLICH, H.. **Thixotropy**. 1935.

[39] GARNER, F. H.; NISSAN, A. H.. **Rheological properties of high-viscosity solutions of lung molecules**. Nature, (158):634–635, 1946.

[40] GIBSON, A. G.; KOTSIKOS, G.; BLAND, J. H. ; TOLL, S.. **Rheological Measurement**. Springer-Science, second edition, 1998.

[41] GODDARD, J. D.; MILLER, C.. **An inverse for the jaumann derivative and some applications to the rheology of viscoelastic fluids**. Rheologica Acta, 5:177–184, September 1966.

[42] GOODEVE, C. F.. **General discussion**. Trans. Faraday Soc., 35(28a-28a), 1939.

[43] GRAESSLEY, W. W.; PRENTICE, J. S.. **Viscosity and normal stresses in branched polydisperse polymers**. Jounal of Polymer Science, 6:1887–1902, November 1968.

[44] GW, S.-B.. **An Introduction to industrial rheology**. Churchill, 1938.

[45] H., G.. **Industrial rheology and rheological structures**. J. Wiley, 1949.

[46] HABIBI, M.; DINKGREVE, M.; PAREDES, J.; DENN, M. M. ; BONN, D.. **Normal stress measurement in foams and emulsions in the presence of slip**. Journal of Non-Newtonian Fluid Mechanics, 238:33–43, 2016.

[47] HAN, C. D.. **Multiphase flow in polymer processing**. Academic Press, 1981. pp. 97-98.

[48] HAN, W.; REDDY, B. D.. **Plasticity Matematical Theory and Numerical Analysis**, volumen 9. Springer-Verlag New York, second edition, 2013.

[49] HARNETT, J. P.; HU, R. Y. Z.. **The yield stress-an engineering reality**. J. Rheol., 33(4):671–679, 1989.

[50] HAYAT, T.; YOUSAF, A.; MUSTAFA, M. ; OBAIDAT, S.. **MHD squeezing flow of second-grade fluid between two parallel disks**. International Journal for Numerical Methods in Fluids, 69(2):399–410, mar 2011.

[51] HILL, R.. **The Mathematical Theory of Plasticity**. Oxford Classic Texts In The Physical Sciences, 1998.

[52] HUYGENS, C.. **De vi centrifuga, in oeuvres complétes**. Vol. XVI:255–301, 1659.

[53] IUPAC. **Compendium of Chemical Terminology**, volumen Version 2.3.3. International Union of Pure and Applied Chemistry - Gold Book, February 2014.

[54] JR., H. R. W.. **Kinetic theory and rheology of dilute suspensions of finitely extendible dumbbells**. Ind. Eng. Chem. Fundamen., 11(3):379–387, 1972.

[55] KEENTOK, M.; TANNER, R. I.. **Cone-plate and parallel plate rheometry of some polymer solutions**. Journal of Rheology, 26:301–311, 1982.

[56] KISS, G.; PORTER, R. S.. **Rheology of concentrated solutions of poly($\beta$-benzyl-glutamate)**. Journal of Polymer Science, 65:193–211, 1978.

[57] KISS, G.; PORTER, R. S.. **Rheology of concentrated solutions of helical polypeptides**. Journal of Polymer Science: Polymer Physics Edition, 18(2):361–388, 1980.

[58] KOSMODAMIANSKII, A. S.. **A new approximate method for the determination of the stresses in an anisotropic plate with a curved aperture**. Some Problems of Elasticity Theory on Stress Concentration and Deformation of Rigid Bodies [in Russian], (2), 1965. Izd. Saratovsk, Unvi., Saratov.

[59] KOTAKA, T.; KURATA, M. ; TAMURA, M.. **Normal stress effect in polymer solutions**. Journal of Applied Physics, 30:1705–1712, 1959.

[60] KOTASA, T.; OSAKI, K.. **Normal stresses, non-newtonian flow, and dynamic mechanical behavior of polymer solutions**. Journal of Polymer Science: Polymer Symposia, (15):453–479, 1967.

[61] KULICKE, W. M.; KISS, G. ; PORTER, R. S.. **Inertial normal-force corrections in rotational rheometry**. Rheologica Acta, 16(5):568–572, Sep 1977.

[62] LARSON, R.. **Arrested tumbling in shearing flows of liquid-crystal polymers**. Macromolecules, 23(17):3983–3992, 1990.

[63] LAUFER, Z.; JALINK, H. L. ; STAVERMAN, A. J.. **Time dependence of shear and normal stresses of polystyrene and poly(ethylene oxide) solutions**. J. Polym. Sci. Polym. Chem. Ed., 11(11):3005–3015, Nov. 1973.

[64] LAUN, H.. **Prediction of elastic strains of polymer melts in shear and elongation**. Journal of Rheology, 30(3):459–501, 1986.

[65] LAUN, H.; RADY, M. ; HASSAGER, O.. **Analytical solutions for squeeze flow with partial wall slip**. Journal of Non-Newtonian Fluid Mechanics, 81(1-2):1–15, feb 1999.

[66] LAUN, H. M.. **Normal stresses in extremely shear thickening polymer dispersions**. Journal of Non-Newtonian Fluid Mechanics, 54:87–108, August 1994.

[67] LEONOV, A. I.; MALKIN, A. Y.. **Effect of normal stresses in steady one-dimensional flows of polymer melts**. Fluid Dynamics, 3:126–129, May 1968.

[68] LODGE, A. S.. **On-line measurement of elasticity and viscosity in flowing polymeric liquids**. Rheologica Acta, 35(2):110–116, Mar 1996.

[69] LODGE, A. S.. **Normal stress differences from hole pressure measurements**, p. 299–326. Springer Netherlands, Dordrecht, 1998.

[70] LUBLINER, J.. **Plasticity Theory**. Macmillan Publishing Company, 1990.

[71] LUU, L.-H.; FORTERRE, Y.. **Drop impact of yield-stress fluids**. Journal of Fluid Mechanics, 632:301–327, 2009.

[72] MACOSKO, C. W.. **Rheology: Principles, Measurements, and Applications**. Wiley, Oct. 1994.

[73] MALKIN, A. Y.. **Normal stresses in non-newtonian polymer flows. 1. calculation of the normal stresses**. Polymer Mechanics, 7:444–450, May 1971.

[74] MALKIN, A. Y.; MASALOVA, I.. **Shear and normal stresses in flow of highly concentrated emulsions**. Journal of Non-Newtonian Fluid Mechanics, 147:65–68, November 2007.

[75] MALKIN, A. Y.; ZABUGINA, M. P.. **Relaxation of normal stresses in flowing polymer systems**. Polymer Mechanics, 11:283–386, March 1975.

[76] MARRUCCI, G.; MAFFETTONE, P.. **A description of the liquid-crystalline phase of rodlike polymers at high shear rates**. Macromolecules, 22(10):4076–4082, 1989.

[77] MATSOUKAS, A.; MITSOULIS, E.. **Geometry effects in squeeze flow of bingham plastics**. Journal of Non-Newtonian Fluid Mechanics, 109(2-3):231–240, feb 2003.

[78] MCMILLEN, E. L.. J. Rheol., 3(75):164–179, 1932.

[79] MEETEN, G. H.. **Effects of plate roughness in squeeze-flow rheometry**. Journal of Non-Newtonian Fluid Mechanics, 124(1-3):51–60, dec 2004.

[80] MEETEN, G. H.. **Squeeze flow of soft solids between rough surfaces**. Rheologica Acta, 43(1):6–16, feb 2004.

[81] MENDELSON, R. A.; FINGER, F. L. ; BAGLEY, E. B.. **Die swell and recoverable shear strain in polyethylene extrusion**. Journal of Polymer Science, 1971.

[82] MERRIAM-WEBSTER. **The Merriam-Webster Dictionary**. Merriam-Webster, Inc., 2005.

[83] METZNER, A. B.; HOUGHTON, W. T.; SAILOR, R. A. ; WHITE, J. L.. **A method for the measurement of normal stresses in simple shearing flow**. Journal of Rheology, 133(5), 1961.

[84] MEWIS, J.; METZNER, A. B.. **The rheological properties of suspensions of fibres in newtonian fluids subjected to extensional deformations**. Journal of Fluid Mechanics, 62:593–600, February 1974.

[85] MEWIS, J.; WAGNER, N. J.. **Thixotropy**. Advances in Colloid and Interface Science, 147-148:214–227, 2009.

[86] MEWIS, J.; WAGNER, N. J.. **Colloidal Suspension Rheology**. Cambridge University Press, 2012.

[87] MISES, R. V.. **Mechanik der festen körper im plastisch deformablen zustand. göttin.** Nachr. Math. Phys., 1:582–592, 1913.

[88] MOLDENAERS, P.; MEWIS, J.. **Transient behavior of liquid crystalline solutions of poly (benzylglutamate)**. Journal of Rheology, 30(3):567–584, 1986.

[89] MORI, Y.; FUNATSU, K.. **On die swell in molten polymer**. Appl. Polym. Symp., 20(209), 1973.

[90] NAKAJIMA, N.; HARRELL, E.. **Normal stresses in flow of polyvinyl chloride plastisols**. Journal of applied polymer science, 103(5):2769–2775, 2007.

[91] NAVARD, P.. **Formation of band textures in hydroxypropylcellulose liquid crystals**. Journal of Polymer Science Part B: Polymer Physics, 24(2):435–442, 1986.

[92] NAWAB, M. A.; MASON, S. G.. **Viscosity of dilute suspensions of thread-like particles**. J. Phys. Chem., 62(10):1248–1253, 1958.

[93] NIGEN, S.. **Experimental investigation of the impact of an (apparent) yield-stress material**. Atomization and Sprays, 15:103–118, 2005.

[94] ODA, K.; WHITE, J. L. ; CLARK, E. S.. **Correlation of normal stresses in polystyrene melts and its implications**. Polymer Engineering & Science, 18:25–28, January 1978.

[95] OLDROYD, J. G.. **A rational formulation of the equations of plastic flow for a bingham solid**. Mathematical Proceedings of the Cambridge Philosophical Society, 43:100–105, 1946.

[96] OSAKI, K.; KIMURA, S. ; KURATA, M.. **Relaxation of shear and normal stresses in step-shear deformation of a polystyrene**

**solution. comparison with the predictions of the doi–edwards theory**. Journal of Polymer Science, 19:517–527, March 1981.

[97] OSSWALD, T. A.; RUDOLPH, N.. **Polymer Rheology: fundamentals and applications**. Hanser Publishers, 2015.

[98] PEDERSEN, S.; CHAPOY, L. L.. **Relaxation of normal and shear stresses after a sudden shear strain in the cone-and-plate experiment using the rheometrics mechanical spectrometer**. Journal of Non-Newtonian Fluid Mechanics, 3:379–388, March 1978.

[99] PELOT, D. D.; SAHU, R. P.; SINHA-RAY, S. ; YARIN, A. L.. **Strong squeeze flows of yield-stress fluids: The effect of normal deviatoric stresses**. Journal of Rheology, 57(3):719–742, may 2013.

[100] PERZYNA, P.. **On the propagation of stress waves in a rate sensitive plastic medium**. Zeitschrift für Angewandte Mathematik und Physik (ZAMP), 14:241–261, 1963.

[101] PETROV, A.; KHARLAMOVA, I.. **The solutions of navier–stokes equations in squeezing flow between parallel plates**. European Journal of Mechanics - B/Fluids, 48:40–48, nov 2014.

[102] PHAM, H. T.; MEINECKE, E. A.. **Squeeze film rheology of polymer melts: Determination of the characteristic flow curve**. Journal of Applied Polymer Science, 53(3):257–264, jul 1994.

[103] POPOV, V. I.. **Relationship between the normal and shear stresses in elastico-viscous liquid flow**. Polymer mechanics, 6:106–109, January 1970.

[104] PRYCE-JONES, J.. 1934.

[105] QAYYUM, A.; AWAIS, M.; ALSAEDI, A. ; HAYAT, T.. **Unsteady squeezing flow of jeffery fluid between two parallel disks**. Chinese Physics Letters, 29(3):034701, mar 2012.

[106] RABIDEAU, B. D.; LANOS, C. ; COUSSOT, P.. **An investigation of squeeze flow as a viable technique for determining the yield stress**. Rheologica Acta, 48(5):517–526, feb 2009.

[107] REINER, M.. **Deformation, strain and flow**. Lewis, London, 1960.

[108] REYNOLDS, O.. **On the theory of lubrication and its application to mr. beauchamp tower's experiments, including an experimental determination of the viscosity of olive oil**. Philosophical Transactions of the Royal Society of London, 177(0):157–234, jan 1886.

[109] ROBERTS, K. D.; HILL, C. T.. **Processability/mechanical properties trade-off for reinforced plastics**. In: PROC. SPE ANNU. TECH. CONF., 31ST PAP., MONTREAL, QUE., p. 536–566, May 1973.

[110] RUSSEL, R. J.. Tese de Doutorado, Imperial College, University of London, 1946. (unpublished), p. 58.

[111] SAIDI, A.; MARTIN, C. ; MAGNIN, A.. **Effects of surface properties on the impact process of a yield stress fluid drop**. Experiments in Fluids, 51:211–224, 2011.

[112] SCHALEK, E.; SZEGVARI, A.. **Ueber eisenoxydgallerten**. Kolloid Z, 318(32):9, 1923.

[113] SCHURZ, J.. **The yield stress-an empirical reality**. Rheol. Acta, 29(2):170–171, 1990.

[114] SHARTS, A. A.. **Temperature influence in use of an interference method to study the effects of normal stresses**. Translated from Zhurnal Prikladnoi Mekhaniki i Tekhnicheskoi Fiziki, 5:177–179, September-October 1977.

[115] SHERWOOD, J.. **Model-free inversion of squeeze-flow rheometer data**. Journal of Non-Newtonian Fluid Mechanics, 129(2):61–65, aug 2005.

[116] SHERWOOD, J.; DURBAN, D.. **Squeeze flow of a power-law viscoplastic solid**. Journal of Non-Newtonian Fluid Mechanics, 62(1):35–54, jan 1996.

[117] SMYRNAIOS, D.; TSAMOPOULOS, J.. **Squeeze flow of bingham plastics**. Journal of Non-Newtonian Fluid Mechanics, 100(1-3):165–189, sep 2001.

[118] STAVROPOULOS, D. N.. **Oxford English-Greek Learner's Dictionary**. Oxford University Press, 1998.

[119] STEFAN, J.. **Versuche über der scheinbare adhäsion**. Sitzungsberichte der Mathematisch-naturwissenschaften Klasse der Kaiserlichen Akademie der Wissenschaften, II. Abteilung, 2(69):713–735, 1874.

[120] STEVENSON, J. F.; BIRD, R. B.. **Elongational viscosity of nonlinear elastic dumbbell suspensions**. Transactions of the Society of Rheology, 15(1):135–145, 1971.

[121] T., P.. **Arch entwicklungsmech org**. (112-160), 1929.

[122] TANNER, R. I.. **A correlation of normal stress data for polyisobutylene solutions**. Transactions of the Society of Rheology, 17:365–373, 1973.

[123] TRESCA, H.. **On further applications of the flow of solids**. Proceedings of the Institution of Mechanical Engineers, 29:301–345, 1878.

[124] VINOGRADOV, G. V.; ISAEV, A. I.; BRIZITSKII, V. I.; PODOL'SKII, Y. Y.; MALKIN, A. Y. ; ZABUGINA, M. P.. **Die swell, normal stresses, and viscoelastic deformations in polymer flow**. Polymer Mechanics, 13:112–117, January 1977.

[125] VINOGRADOV, G. V.; MALKIN, A. Y.; BEREZHNAYA, G. V.; BOSTANDZHIYAN, S. A. ; STOLIN, A. M.. **Normal stresses associated with the flow of non-newtonian polymer systems. 2. experiment and comparison with theory**. Polymer Mechanics, 7:633–639, July 1971.

[126] VINOGRADOV, G. V.; MALKIN, A. Y. ; SHUMSKY, V. F.. **High elasticity, normal and shear stresses on shear deformation of low-molecular-weight polyisobutylene**. Rheologica Acta, 9:155–163, April 1970.

[127] WEISSENBERG, K.. **A continuum theory of rhelogical phenomena**. Nature, 159:310–311, 1 March 1947.

[128] WHELAN, T.. **Polymer Technology Dictionary**. Springer, 1994.

[129] WILLIAMS, M. C.. **Concentrated polymer solutions: Part iii. normal stresses in simple shear flow**. AIChE Journal, 1967.

[130] XU, J.; COSTEUX, S.; DEALY, J. M. ; DE DECKER, M. N.. **Use of a sliding plate rheometer to measure the first normal stress difference at high shear rates**. Rheologica Acta, 46(6):815–824, Jun 2007.

[131] YANG, S.-P.; ZHU, K.-Q.. **Analytical solutions for squeeze flow of bingham fluid with navier slip condition**. Journal of Non-Newtonian Fluid Mechanics, 138(2-3):173–180, oct 2006.

[132] ZIMM, B. H.. **Dynamics of polymer molecules in dilute solution: viscoelasticity, flow birefringence and dielectric loss**. The Journal of Chemical Physics, 24:269–278, 1956.

[133] ZIRNSAK, M. A.; HUR, D. U. ; BOGER, D. V.. **Normal stresses in fibre suspensions**. Journal of Non-Newtonian Fluid Mechanics, 54:153–193, August 1994.

# A
# Squeeze flow with no-slip boundary condition

A rotational shear stress controlled and Peltier temperature controlled rheometer[1] was employed. In order to reproduce approximately the no-slip boundary condition, parallel cross-hatched plates with 60 mm of diameter were adopted. Furthermore, instead of full fill the gap between plates, a centralized coaxial cylindrical mold was designed and used with 20 mm of diameter and 15 mm in height. Although it is not possible to ensure perfect no-slip boundary condition, a very close condition was obtained, as can be seen in Figure A.1, in which the plate effect on the sample is noticeable and symmetric. The experimental procedure adopted pursues the following steps: (a) set and calibrate the initial gap and other parameters, (b) fit the mold on the bottom plate of the rheometer, (c) place the material with a syringe, (d) eliminate excess material, (e) eliminate blisters with the syringe, (f) remove the mold, (g) set the upper plate in contact with the top of the sample and, (h) fit a chamber to avoid evaporation.

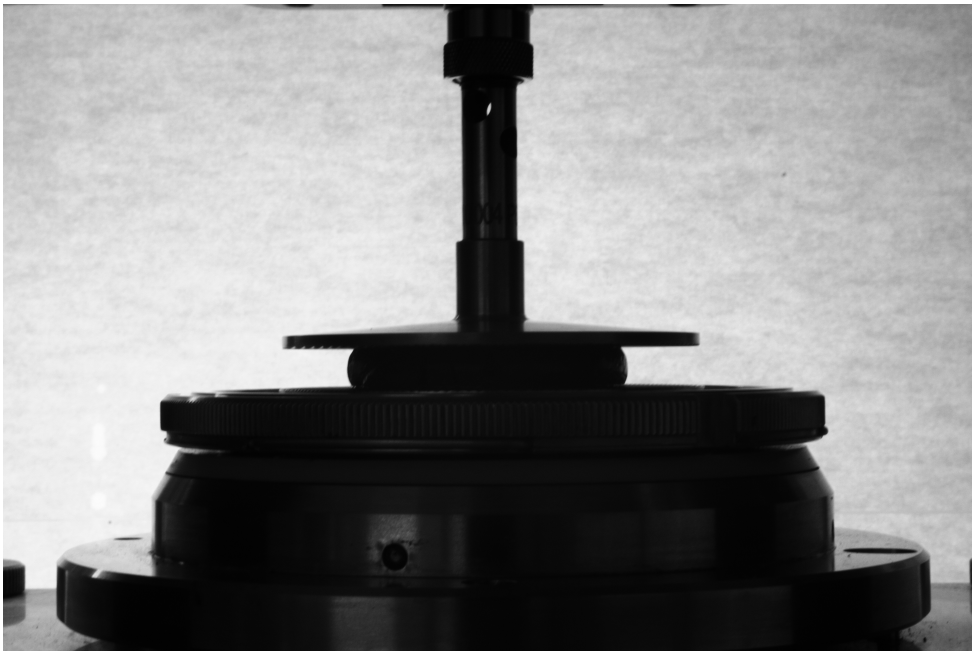

Figure A.1: Constant volume squeeze flow test.

[1]Haake Mars III.

Constant volume squeeze flow tests were performed, specifically, a constant normal force experiment was employed and the gap separation between plates was recorded over time. It was considered an absolute value of 1 N for the normal force, except for the putty in which an absolute value of 2 N was considered instead, due to its consistency. It was possible to reach static equilibrium state for all materials analyzed. The results are shown in Figures A.2 and A.3. The critical stresses ($\sigma_{11,y}$), defined as the ratio between the applied normal force and the current cross-section area of the sample measured at the static equilibrium condition, are shown in Tables A.1 and A.2. The current cross-section area could be obtained by simple geometry because the experiment is volume preserving due to special chamber adopt to avoid evaporation.

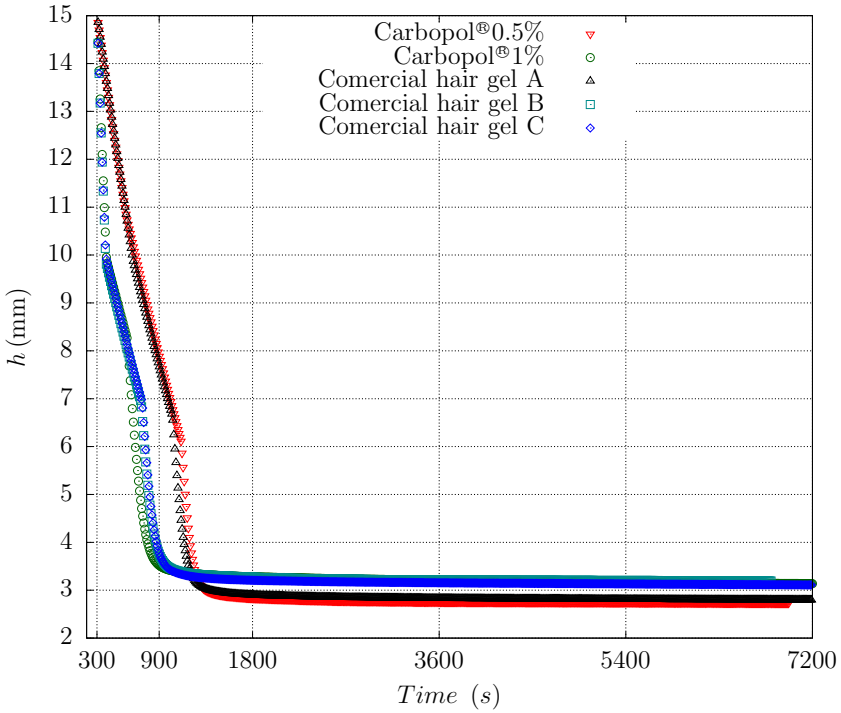


Figure A.2: Gels behavior under a constant volume squeeze flow test, with no-slip boundary condition.

Table A.1: In this table we show for each gel analyzed in this work: the yield strengths and critical lengths for a no-slip boundary condition.

| Materials | $\sigma_{11,y}$ (Pa) | Critical length (mm) |
|---|---|---|
| Carbopol® 0.5% | 579.32 | 2.73 |
| Carbopol® 1.0% | 664.21 | 3.13 |
| Comercial hair gel A | 592.06 | 2.79 |
| Comercial hair gel B | 676.94 | 3.19 |
| Comercial hair gel C | 657.84 | 3.1 |
| **No-slip constant volume squeeze flow - Gels** | | |
| Initial gap ($mm$) | 15 | |
| Initial diameter ($mm$) | 20 | |
| Cross hatched plates diameter($mm$) | 60 | |

For all gels, the gap profile over time exhibited a similar qualitative behavior (figure A.2). For simplicity, we are going to call group I the materials: Carbopol® 1.0%, commercial gel B and C, and group II the materials: Commercial gel A and Carbopol® 0.5%. The behavior of the gap separation between plates profile over time exhibited the following tendencies: (i) for the group I, the gap profile displayed a dramatic drop of approximately 5 mm high, then a monotonic linear decreasing behaviour followed by another critical drop with a smooth transition to an asymptotic value, indicating that the materials have reached the static equilibrium; and (ii) for the group II, a more behaved profile was observed in which a monotonic linear decreased until 6.5 mm high when an increase in angle takes place with and smooth transition until achieved an asymptotic behavior which indicates that the materials have reached the static equilibrium. Moreover, it was observed that the gels analyzed have taken near to 30 minutes to achieve the static equilibrium state consistently.

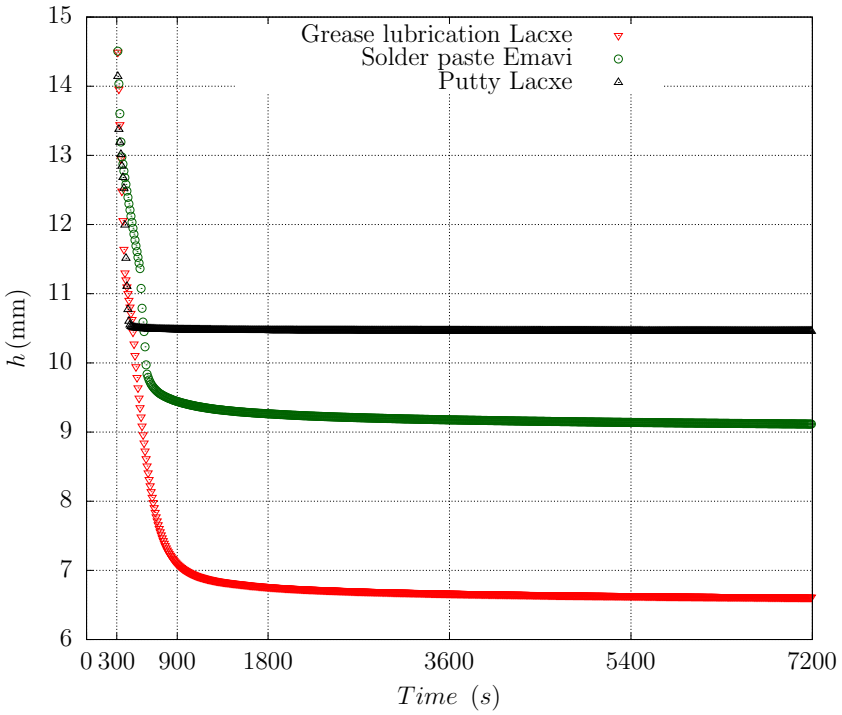


Figure A.3: Pastes behavior under a constant volume squeeze flow test, with no-slip boundary condition.

Table A.2: In this table we show for each paste analyzed in this work: the yield strengths and critical lengths for a no-slip boundary condition.

| Materials | $\sigma_{11,y}$ (Pa) | Critical length (mm) |
|---|---|---|
| Grease lubrication | 1402.69 | 6.61 |
| Solder paste | 1933.20 | 9.11 |
| Putty | 4439.36 | 10.46 |
| **No-slip constant volume squeeze flow - Pastes** | | |
| Initial gap $(mm)$ | 15 | |
| Initial diameter $(mm)$ | 20 | |
| Cross hatched plates diameter$(mm)$ | 60 | |

Considering the gap separation between plates profile recorded over time, for pastes, different behaviors among themselves were observed (figure A.3). Each behavior presented the following tendencies: (i) the solder paste gap profile displayed a dramatic drop of approximately 2 mm in height, then a monotonic linear decreasing behavior followed by another critical drop with a smooth transition to an asymptotic value, indicating that the material has reached the static equilibrium; (ii) a sharp linear monotonic decrease with a smooth transition to an asymptotic value was displayed by the grease gap profile and; (iii) The putty gap profile displayed a dramatic drop of

approximately 4.5 mm high direct to an asymptotic value. Moreover, the pastes have taken near to an hour and 30 minutes to achieve the static equilibrium condition consistently. The compressive critical stresses for each paste are shown in Table A.2.

It was possible to obtain the static equilibrium under no-slip boundary condition for several elasto-viscoplastic materials, including gels and pastes. As expected the critical stresses estimated are lower than those previously obtained for the partial slip case (see section 4.1), which seems reasonable due to the additional resistance caused by the accumulation of material inside the gaps of the cross-hatched plates. Unfortunately, due to the complex nature of this flow, it was not possible to estimate the yield stress using von Mises theory.